SKB

TECHNICAL REPORT 91-55

Redox capacity of crystalline rocks. Laboratory studies under 100 bar oxygen gas pressure

Veijo Pirhonen, Petteri Pitkänen

Technical Research Center of Finland

December 1991

SVENSK KÄRNBRÄNSLEHANTERING AB
SWEDISH NUCLEAR FUEL AND WASTE MANAGEMENT CO
BOX 5864 S-102 48 STOCKHOLM
TEL 08-665 28 00 TELEX 13108 SKB S
TELEFAX 08-661 57 19

REDOX CAPACITY OF CRYSTALLINE ROCKS. LABORATORY STUDIES UNDER 100 BAR OXYGEN GAS PRESSURE

Veijo Pirhonen, Petteri Pitkänen

Technical Research Center of Finland

December 1991

REDOX CAPACITY OF CRYSTALLINE ROCKS

Laboratory studies under 100 bar oxygen gas pressure

Veijo Pirhonen, Petteri Pitkänen

Technical Research Center of Finland

December 1991

This report is also published in the TVO report series

ABSTRACT

The excess amount of dissolved oxygen has been used as a reducible species in order to determine reducing ability (redox capacity) of crystalline rocks and minerals in an aqueous granite solution. Both crushed and whole rock samples were used. The oxygen pressure was set to 100 bar both to promote diffusion and accelerate the surface reactions. The redox capacity was obtained as a function of the decrease of Fe (II) in the solid phase. The decrease of ferrous iron near the reaction surface ranged from about 2 % up to 39 %. All reacted samples showed a decrease of between 5 - 30 % in the ratio of $FeII/Fe_{total}$ within a reaction zone at the rock surface. The reaction depth varied from about 0.1 cm up to more than 2.5 cm in rocks that were artificially ruptured and in naturally fractured granitic rocks, respectively. The redox capacity calculated from the average decrease of iron in profile varied from about 18 to 620 mol_{FeII}/m^3 and 320 to 580 mol_{FeII}/m^3 for the ruptured and the natural fracture samples, respectively.

PREFACE

This work has been done in the Technical Research Centre of Finland (VTT) and financed by Svensk Kärnbränslehantering Ab (SKB) and Teollisuuden Voima Oy (TVO). The contact persons have been Dr. Peter Wikberg (SKB), MSc Marcus Laaksoharju (SKB), Tech. Lic. Jukka-Pekka Salo (TVO), Dr. Juhani Vira (TVO), Dr. Veijo Pirhonen (VTT) and MSc Petteri Pitkänen (VTT). Marcus Laaksoharju, and Dr. Steven Banwart from the Royal Institute of Technology (RIT) have partipated evaluation and design of the experiments, professors Ingemar Grenthe and Ivars Neretnieks have critically rewied the earlier status reports and drafts. Their support is acknowledged with great gratitude. The authors are especially indepted to Dr. Antti Vuorinen from the University of Helsinki (HY), who has given his great expertise for making the iron analyses possible. The figures were drafted by Mr. H. Jukka and the text was edited by Mrs. Anneli Asunta and Mrs. Tuula Streng. Contributions of all the other fellow workers in the VTT and the HY are also appreciated.

CONTENTS

1 INTRODUCTION

THE OBJECTIVE of the present redox experiments was to measure reducing capacity resulting from oxidation of ferrous iron in the granitic rocks and minerals. This was done by exposing rock and mineral samples to aqueous solution under O_2 athmosphere, and measuring decrease in ferrous iron contents. The possibility of parallel dissolution of iron was also examined. This is essential in order to estimate contribution of rock to the processes that can consume oxygen in the oxygen bearing zone of a redox front resulting from radiolysis.

Different rock types like metabasite, diorite, granodiorite, tonalite, mica gneiss, and granite have been examined (Table 1). Rocks with natural fracture surfaces were compared with artificially ruptured or polished rock surfaces to see if there is any physical effect on the reactivity. The samples represent different rock forming conditions, and deformation and weathering histories. Variations of ferrous iron contents are expected to have an important effect on the experimental results.

Table 1. Types and locations of fracture (a) and intact (b) rock samples.

Rocktype	Borehole/ sample code	Area	Section (m)	Deformation/ alteration/ weathering 1)	Relative FeII contents
(a)					
Mica gneiss I	OL-KR2	Olkiluoto	490.29 - 491.08	D/A/AUW	moderate
Tonalite	SY-KR3	Syyry	454.25 - 455.00	D/MA/UW	moderate
Mica gneiss II	SY-KR5	- " -	697.25 - 697.97	D/MA/UW	moderate
(b)					
Äspö metadiorite	Kas 02-1	Äspö	756.00 - 757.00	D/A/UW	low
Smålands granite	Kas 02-2	- " -	158.00 - 159.00	H-D/MA/UW	lowest
Granodiorite I	Fi8-1	Finsjön	231.00 - 231.82	D/A/UW	moderate
- " - II	Fi8-2	- " -	250.73 - 251.29	H-D/MA/UW	moderate
Metabasite	Fi4	- " -	119.45 - 119.96	H-D/UA-MA/UW	high

1) D = deformed, H = homogeneous, A = altered, MA = moderately altered, UA = unaltered, W = weathered, UW = unweathered

2. MATERIALS AND PROCEDURES

2.1 Sample material

In this chapter a petrographic description of the sample material is given, refering to both intact rock samples (for determining average petrographic features), and fractured samples (for studying possible mineralogical and/or structural changes in the vicinity of the fractures). The rock samples are drilled cores, the types and sampling

locations are presented in Table 1. Descriptions are given also for mineral specimens (hypersthene, olivine, hornblende, biotite, muscovite, pyrite, and magnetite) which were taken from outcrops and mines. The mineral compositions of the rocks used in this study are presented in Table 2. and the photographs of the prepared samples are shown in Appendix 2.

2.1.1 Natural fracture samples

Mica gneiss OL-KR2

When observed on the mesoscopic scale, the rock has a dark gray colour caused by the medium grained mixture of plagioclase, quartz and biotite. This main content is irregularly cut by a brighter, coarse grained granitic vein which contains large crystals of mainly plagioclase and quartz. In the macroscale, The granitic veins cause heterogeneity to the rock but, however, the mica gneiss which makes the bulk volume of the rock, can be regarded as homogeneous.

Obtained by microscope, the main primary minerals are plagioclase, quartz and biotite, which together make about 85 % of the total rock volume. Secondary minerals are sericite (after plagioclase alteration), chlorite (after biotite), and carbonate (probably calcite) which occurs mainly as a fracture filling. Accessories are zircon, white mica, opaques and clay. The gneissic features are strong but, however, the distribution of the minerals in the rock seems to be homogeneous.

The main fracture surface (Appendix 2.8) is parallel to the micas orientation (gneissic) and is coated by carbonate which is accompanied with fine quartz (precipitated?) and some type of clay. The fracture coating has a width of 0.2 - 0.5 mm. In the midsample, a large carbonate filled fracture (Appendix 2.9) having a width of 0.1 - 0.5 mm appears

together with fine quartz, it is elongated (few mm) and parallel to the main fracture surface. Short carbonate filled diffusion channels develope at some locations along it. Other fractures of the same type but much smaller in scale, appear with a same orientation inside some of the medium-large quartz and plagioclase grains. At the near zone, up to a distance of 3 - 5 mm from the main fracture surface and the large carbonate filled midsample fracture, it can be clearly seen that biotite had lost its pleochroic green colour during its alteration to chlorite, and that plagioclase had strongly altered to sericite. The two dominant fractures and their associated altered minerals, in relation to the non-altered parts of the sample, make a zonal appearance of separated fresh and altered stripes, all, in the same orientation. The coarse-grained granite vein seems to have caused the biotite grains to partly alter into chlorite. This process is believed to have been taken place at locations far enough from possible fracture influence. Other carbonate filled, intergrain microfractures with an orientation which is different from the above, are located inside few plagioclase grains of the granite vein. Fluid inclusion rims in quartz grains (Appendix 2.10) are common throughout the sample, they seem to have an orientation which is similar to the general texture (gneissic) and the main fractures.

Tonalite SY-KR3

When observed on the mesoscopic scale, the rock has a light gray colour caused by the high amount of plagioclase and quartz grains which are mixed together with a low content of biotite and hornblende. The rock is oriented (gneissic) and in general, looks homogeneous. Two perpendicular fracture surfaces are present, they are clearly altered and coated by a green mixture of chlorite and some type of clay. The shorter of the two surfaces is in addition, coated by some 1.0 mm thick of carbonate cover (probably calcite).

Observed by microscope, the main primary minerals are plagioclase, quartz, biotite and hornblende. The first two are medium to very coarse (5 mm) and cause a porphyritic appearance. All hornblende crystals are strongly altered. Together, the primary minerals make more than 90 % of the total rock volume. Secondary minerals are sericite, epidote and carbonate after plagioclase alteration, and chlorite after the alterations of biotite and hornblende. Accessories are zircon and opaques. The biotite is distributed in concentrated zones of fine-medium flakes but, the rock in general, appears as homogeneous.

The (longer) fracture surface and the general orientation (gneissic) of the micas are parallel. In the near zone (1 - 2 mm) of the two (perpendicular) fracture surfaces, it seems likely that biotite flakes have altered to chlorite (Appendix 2.11) and perhaps, as a further step, also to some type of clay. An intergrain fracture filled with very fine quartz precipitation and some chlorite, appears to cut plagioclase grains in a direction which is parallel to the (longer) fracture surface. This fracture is some 3-4 mm long and of about 0.05 mm thick. Inter and intragrain microfractures with very low spacing if at all, are present in many of the plagioclase grains, some of them have an extension into neighbouring quartz grains. Fluid inclusion rims in quartz grains are also present.

Mica gneiss SY-KR5

Observed on the mesoscopic scale, the rock has a dark gray colour, caused by the relatively high amount of biotite flakes (25%) which are sited among plagioclase and quartz grains. In general, the rock is medium-grained, equigranularic, oriented (gneissic or foliated) and homogeneous.

Observed by microscope, primary minerals are quartz, plagioclase, biotite and muscovite, they together make about 97 % of the total volume and thus, the rock can be regarded as fresh. Secondary minerals are sericite, epidote and chlorite which are present as accessories and formed by the (partly) alteration of plagioclase and biotite. Other accessories are apatite, zircon and opaques. Poikiloblastic texture occurs, it was caused by fine quartz inclusions in muscovites. Fluid inclusion rims (Appendix 2.12) in quartz grains are common and by which some of, may have an extension over neighbouring (quartz) grains. Carbonate filled fractures occur at some locations in the sample (Appendix 2.13).

2.1.2 Artificially ruptured or polished samples

Äspö metadiorite Kas 02-1

On the mesoscopic scale, the rock has a dark gray colour caused by the medium grained mixture of plagioclase, quartz, potassic feldspar and biotite. Large lighter spots are due to feldspar megacrysts in which at least some of them are metamorphic (Wikman et al., 1988), the distribution in the rock of these larger grains seems to be slightly heterogeneous. Orientation is clearly present and the rock should be referred to as porphyroblastic metadiorite.

Observed by microscope, main primary minerals are plagioclase, quartz, microcline and biotite, these together, make no more than 65% of the total rock volume. The rock is relatively rich in secondary minerals such as sericite, epidote and carbonate, all formed by the advance alteration of plagioclase. Accessory minerals are sphene (both primary and secondary), apatite, zircon, allanite and opaques.

Carbonate-filled intergrain fractures some 2 mm thick, occur inside large plagioclase grains. At some locations they may extend into neighbouring quartz or microcline crystals where

no carbonate filling is visible. Carbonate fractures are low intensity in colour and occur only at few locations. Long (few millimetres) intergrain non filled fractures with a very limited spacing, if at all, occur and extend through several grains of plagioclase, quartz and microcline (Appendix 2.14). In general, these are parallel to the carbonate filled-fractures, and may together with them, belong to one single (fracture) system. Other common features are the high intensity of shear zones, filled mainly by fine grains of quartz, and the fluid inclusions in medium-large grains of this mineral.

Smålands granite Kas 02-2

On the mesoscopic scale, the rock has a light gray colour caused by the high amount of plagioclase, quartz and potassic feldspar. Grains of the latter are large (megacrysts) and due to some iron content, appear with reddish colour. Black spots are caused by low amount of biotite. In general, the rock is oriented (gneissic) and looks homogeneous.

Observed by microscope, primary minerals are plagioclase, quartz, microcline and biotite, which together make about 90 % of the total rock volume. Sericite, epidote and carbonate are the secondary minerals after plagioclase alteration. Accessory minerals are apatite, sphene (both primary and secondary), zircon and opaques. The texture is somewhat porphyritic due to the large feldspar crystals. Perthite, granophyre and myrmekite textures are common. Intergrain microfractures with very low spacing, if at all, occur in some of the large feldspar grains. In few locations they have a high frequency appearance of some 2 fractures/mm. Intragrain microfractures with no spacing occur inside large plagioclase crystals. Fluid inclusions in medium-large quartz grains are common, some of them have an extension into neighbouring (quartz) grains. Shear zones, filled mainly by fine quartz are also common.

Granodiorite Fi8-1

On the mesoscopic scale, the rock is dark coloured due to the relatively high amount of biotite and hornblende crystals, which are sited among the lighter grains of feldspar and quartz. Some areas contain lots of hornblende and thus, cause some heterogeneity in the rock. Orientation is visible.

Observed by microscope, the main primary minerals are plagioclase, quartz, microcline, hornblende and biotite which together make about 80% of the total rock volume. Secondary minerals are sericite (major) and epidote after the advance alteration of plagioclase, and minor amount of chlorite (after biotite). Accessory minerals are zircon and sphene. In general, the rock is medium to large grained, poikilitic hornblendes are common and some orientation is present. Fluid inclusions and microfractures (Appendix 2.15) in quartz grains are very common.

Granodiorite Fi8-2

On the mesoscopic scale, the rock appears as medium-large grained, equigranularic and with some orientation (gneissic). Mafic-rich zones (few centimetres) are present and cause heterogeneity.

Obtained by microscope, the main primary minerals are plagioclase, quartz, microcline, hornblende and biotite which together make more than 90 % of the total rock volume.

Secondary minerals are sericite and epidote after plagioclase alteration, and chlorite (minor amount) after biotite. Accessories are apatite, zircon and (secondary) sphene. Hornblende crystals are poikilitic. Perthite, antiperthite and myrmekite textures are common.

Long (several millimetres) intergrain microfractures of low intensity and with a very limited spacing (microns), and some fluid inclusions are present in quartz grains. Few intragrain microfractures, occur inside hornblende crystals.

In general, FI8-2 and FI8-1 rock samples, which are taken from same borehole, are similar. They somewhat differ only in their hornblende content and the rate of plagioclase alteration (sericite content).

Metabasite (metadiabase) Fi4

On the mesoscopic scale, the rock appears as medium grained and equigranularic, it has a dark black colour (mafic rich) and seems to be homogeneous.

Observed by microscope (Table 1), primary minerals are hornblende (50 %), plagioclase, quartz, biotite and microcline which together make about 95 % of the total rock volume. Secondary minerals are sericite and epidote (after plagioclase) and some chlorite (after biotite). Accessories are sphene, apatite, zircon and opaques. Obtained from two different locations along the core sample, various rates of seritization of plagioclase and chloritization of biotite are found, this may leed to the conclusion that the alteration is not at the same level throughout the rock.

No significant changes of any kind are visible along the polished surface. Intragrain microfractures with no spacing are present in plagioclase grains. They appear with low intensity. Also present are fluid inclusions in quartz.

Table 2. Modal mineral distributions (%) of rock samples.

	Mica-gneiss I	Tonalite	Mica-gneiss II	Meta-diorite	Granite	Grano-diorite I	Grano-diorite II	Meta-basite
Plag.	39,9	59,1	26,2	26	32	21,7	38,9	25,4
K-feld.				11,5	24,9	7,4	6,9	2
Quartz	34,6	21,8	31,4	13,1	28,2	21,2	25,3	10,1
Biotite	11,5	10	25	15,8	5,8	11,7	9,3	6,5
Chlorite	3	1,1	+			+	+	+
Muscovite	1		14,1					
Hornbl.		4				19,8	11,7	50
Epidote		1,3	+	11,5	2	3,6	2,7	2,2
Calcite	1,5	+		3	+			
Sericite	7	2	+	14,7	3,1	13,4	3,1	1
Apatite			1	1	+		1,2	+
Zircon	+	+	+	+	+	+	+	+
Sph./Leoc				2	1,2	+	+	1,1
Allanite				+				
Clay	+							
Opaques	1	+	1	1	2			+
Fe II cont.	moderate	moderate	moderate	poor	poor	moderate	moderate	rich

2.1.3 Mineral samples

Hypersthene

The sample is purely consisting of hypersthene (very large crystal). In addition to the typical cleavage, large and elongated (few millimetres) fractures (Appendix 2.16) are cutting the rock. Probably, these have some spacing which allowed aqueous solutions to react with the mineral and oxidise it. More intensive system of intergrain fractures appears, and has a very limited spacing, if at all. When combining the two fracture systems, the average diameter of

the nonfractured area which lies among them, is of some 0.5 - 1.0 mm. In comparison to the inner parts, the margins of the sample are intensively broken and cracked.

Olivine

On the mesoscopic scale, the sample, which is purely consisting of olivine (very large crystal) has a light green colour and when observed by microscope no pleochroic colours are visible, therefore, it is assumed to have low iron content. The crystal is intensively fractured by inter and intragrain microfractures in which some of, may have a limited spacing (microns). The average diameter of the nonfractured area which lies between the above, is of some 1.0 mm in diameter. Opaque dust is common throughout the sample and has a homogeneous distribution.

Hornblende

On mesoscopic scale, this hornblende-rich rock sample appears as medium-large grained, equigranularic, dark-black coloured and oriented (gneissic).

Observed by microscope, the main primary minerals are hornblende (83.1%), plagioclase and biotite which together make more than 95% of the total rock volume. Sericite is the only secondary mineral after the (partly) alteration of plagioclase. Accessories are zircon and opaques. Hornblende crystal fractures are clearly visible and they appear with high intensity.

Biotite

Extremely large (several tens of centimetres) crystals of biotite apparently originate from a granite pegmatite. When observed by microscope, the pleochroic colour is green and very strong, thus, reflecting high iron/magnesium ratio.

Muscovite

Extremely large (several tens of centimetres), colourless crystals of muscovite apparently originate from a granite pegmatite complex.

Pyrite

Very large and pure aggregate of medium grained, equigranularic crystals of pyrite.

Magnetite

Large, dark-black and massive sample of very fine-fine grains of magnetite, an obvious banded formation.

2.1.4 Porosity

The porosity profiles of natural fractures are as follows:

The porosity profiles of the three fracture samples (Appendix 3), are clearly decreasing within the first 10 mm from the fracture surface. OL-KR2 and SY-KR5 samples have fracture surfaces which appear differently, however, they are both having composition and texture of a mica gneiss which may explain the similarity exhibited by their porosity profiles. Thus, the rock type may have a strong influence on the porosity profile. The porosity profile of the tonalite SY-KR3 sample is parabolic and decrease from the high value of 0.80 % at 1.5 mm from the fracture surface, down to 0.32 % at a distance of 10.4 mm. It can be clearly seen that the presented profile of this sample has, at any distance, higher porosity values than those presented in the profiles of OL-KR2 and SY-KR5 (mica gneiss) samples.

The fracture samples have clear porosity interfaces where porosity decreased from the surface (0.32-0.8 % vol) towards

the matrix (0.1-0.3 % vol) within a distance of 0.5 to 1.0 cm from the surface (Appendix 3).

Porosity of rock samples:

The porosity values (Table 3) of the granodiorite, diorite, aplite and metabasite (FI8-1, KAS02-1, FI8-2 and FI4 samples, correspondingly) are low and similar, all, in the range of 0.06 - 0.09 %. Different from these, is the granite KAS02-2 sample which has a porosity value of 0.18 % which is as twice high as the maximum value of the above range.

Table 3. Porosity of fracture profiles (a) and porosity and surface area of rock and mineral samples (b).

a.

Sample	Distance from surface (mm)	Effective porosity (vol. %)
1. Mica gneiss I		
OL-KR2-1	1.9	0.32
-2	5.9	0.18
-3	9.6	0.11
2. Mica gneiss II		
SY-KR5-1	2.5	0.21
-2	7.4	0.17
-3	9.6	0.09
3. Tonalite		
SY-KR3-1	1.5	0.80
-2	5.6	0.46
-3	10.4	0.32

b.

Sample	Rock name	Porosity (%)	Surface ares (m^2/g)
FI8-1	granodiorite I	0.08	1.0
FI8-2	granodiorite II	0.07	1.0
FI4	metabasite	0.06	
Kas 02-1	Äspö diorite	0.09	
Kas 02-2	Småland granite	0.18	
Minerals	hy, ol, hbl, bt, mcv, py, mgt		1.0...5.0

2.2 Sample preparation

Sample preparation and treatment of all the samples is illustrated in Figure 1. To prepare pulverised rock that was used in the test run, rock cores were crushed with jaw-crusher (jaws were covered with PETP-fabric). Smaller pieces were ground in an agate mortar and pulverised in quartz ball mill for 30 min. Samples were sieved to -100 +200 mesh size. Stainless steel sieves were used. Measured Baum-Emmet-Teller (BET) average surface area value of the sample is 0.91 - 1.0 m^2/g for rock pulver and up to 4.0 m^2/g for ground minerals (Table 3). Crushing, grinding and sieving were carried out in a glove box pressurised with nitrogen gas. Samples were emplaced in PVC-containers for transportation and further emplacement in a reaction vessel.

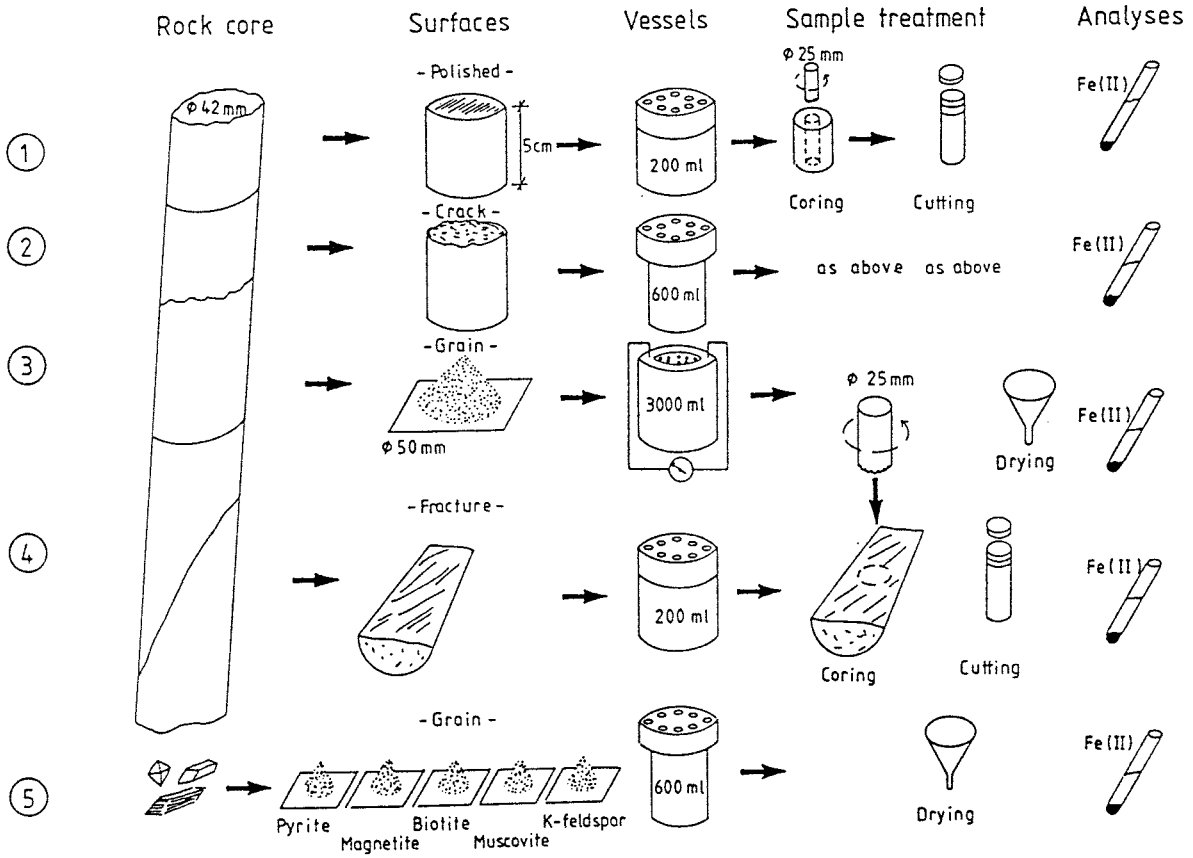

Figure 1. Schematic illustration of sample preparation and treatment procedures.

The whole rock samples were original drill cores with diameter of 42 mm. The cores were sawn or ruptured into 50 mm long pieces. All the surfaces were sealed with silicon, except the reaction surfaces on the top of the core pieces.

The reaction surfaces were either natural, or prepared in order to examine possible variations in reaction ability and the widths of the forming reaction fronts in the samples. The redox capacity (reducing ability) of the samples is expected to vary as follows:

(1) A pulverised sample has a great reaction surface area. This type of sample represents the maximum redox capacity of rock, or mineral.

(2) On polished rock surfaces, mineral defects (cracks and pores) are reduced, the reaction surface area is in the minimum, and a diffusion interface between the surface and rock matrix should be restricted. Polished samples were expected to represent the minimum redox capacity of rocks.

(3) Artificially ruptured rock samples represent the fractures (cracks) around excavations. Their diffusion interfaces are expected to consist mainly of microfractures. These sample represent the maximum volume of redox capacity per specific surface of rock.

(4) The natural fractures are surrounded by characteristic diffusion interfaces (Pirhonen et al. 1990). Natural fractures may represent partially passivated surfaces described by White and Yee (1985). These samples may represent the redox capacity of natural specific surface of rock.

2.3 Oxidation experiments

The samples were oxidized in autoclaves (Figures 1 and 3). Three different types of (autoclaves) reaction bomb were used. The test runs # 1 - 2 with pulverised granodiorite, in contact with synthetic granite type water (Appendix 4), were done at ambient conditions in the 3000 ml titanium autoclave equipped with an online oxygen sensor (Figure 2). At the beginning of the experiment oxygen loss and cation contents were followed (Appendices 5 and 6). When the system was equilibrated, in about a month samples were taken from solution and the solid phase, and the vessel was pressurised with oxygen. The pressure was increased up to 100 bar by adding oxygen gas into the vessel. The tests were terminated and the Fe (II) of the final solids was analyzed two months later.

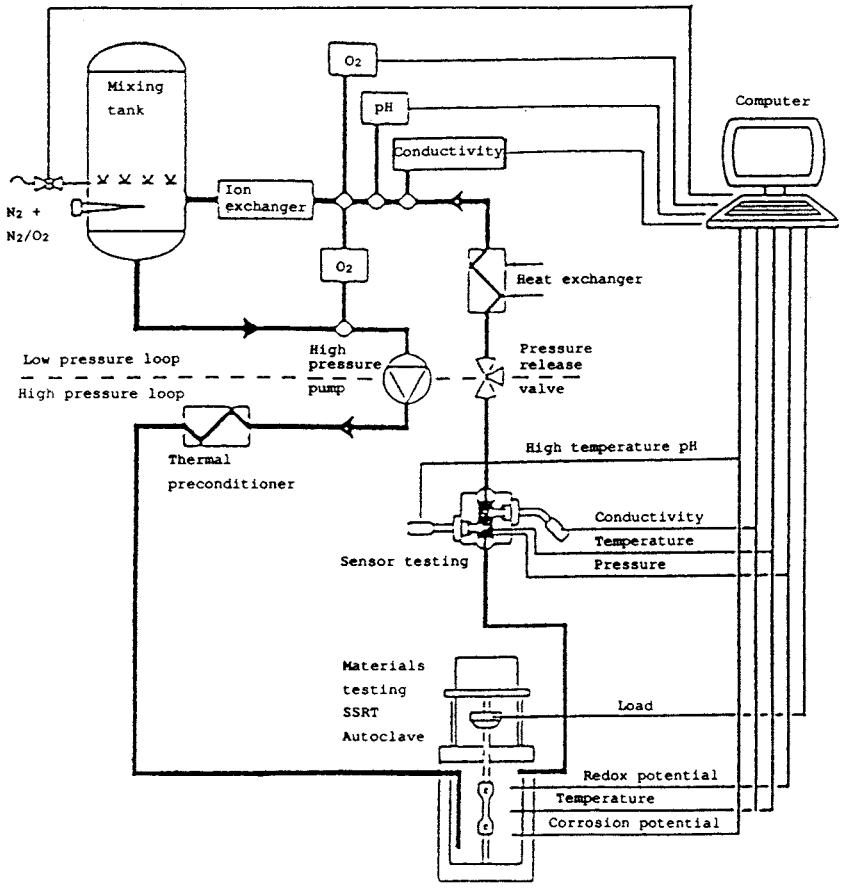

Figure 2. 3000 ml flow-through autoclave with on line corrosion resistivity and pH measurement system. Different lining materials available.

Most of the whole rock samples were oxidized at the same time. The samples were closed in 3000 ml vessel and oxidized in water at 100 bar of O_2 for four month, except the pilot test with ruptured (crack) samples, that were oxidized in 600 ml autoclave for 3, 6 and 10 weeks.

2.4 Diffusion profiles

The diffusion profiles describe the distance from the reaction surface that is affected by dissolved oxygen. This is measured as a function of decrease of Fe (II) in rock, and expressed also as variation of Fe (II)/Fe_{tot} ratio as a function of the distance from the reaction surface.

The analysed samples were sliced from cylinders, diameter 15 mm, cored perpendicular to the reaction surface. The thickness of the slices in the natural samples was approximately 1 mm and varied from 1 to 5 m in treated samples.

The sliced pieces were crushed, ground, and treated as the pulverised samples (see chapter 2.2). Each slice in the profiles was analysed separately.

A modified version of the micro-analytical colorimetric method (a volumetric technique) developed by WILSON (1960) for determination of Fe (II) in silicate minerals and rocks was used. A more detailed description of the technique is given in Appendix 1. Magnetite and pyrite, was analysed with Mössbauer spectroscopy technique (DRYAR ET AL. 1987). The total iron content of the solids was analysed with Atomic Adsorption Spectroscopy (AAS). The Fe_{tot} and HCO3- of the solution were analysed both at the beginning and at the end of the experiment, with the Induced Coupled Plasma spectroscopy (ICP) and titration techniques correspondingly.

When using the volumetric method one should be aware of the scaling error that may occur due to variation of conditions in different sample series. This is rather common to most of the wet-chemical methods. The profiles should be normalized according to the last analysis point in the profile, if it can be expected to represent the original iron contents of rock. Otherwise, oxidized samples can only be compared to a separately analyzed homogeneous background sample.

Variations caused by heterogeneties of rock can be examined by analyzing unreacted background samples. About ten pieces of 1 to 3 mm thick samples per background profile should be sufficient.

3. RESULTS

3.1 Iron contents of rock before and after oxidation

All reacted samples showed a decrease of between 5 - 30 % in the ratio of $FeII/Fe_{total}$ within a reaction zone at the rock surface. The results for the artificially ruptured samples are shown in Figure 3. These samples all showed a well-defined reaction layer of 1 cm depth or less, with ferrous iron contents decreasing from the background concentration in the direction of the rock-solution interface.

This concentration gradient is very pronounced in the metabasite. The other three samples are all granitic and show less dramatic decrease in ferrous iron. One difference between metabasite and the granites is the source of reactive iron; hornblende is the predominant FeII mineral in metabasite whereas biotite is the iron bearing phase in the granites, except Granodiorite I, where also heterogeneously distributed hornblende occurs.

The results for the samples with natural fracture surfaces are shown in Figure 4. The decrease in $FeII/Fe_{total}$ ratio is

generally 20 - 30 % throughout the measured profiles. These extend to distances of 14 mm into the rock sample. It was not possible to determine the extent of the reacting layer due to the size restrictions of the samples.

The deeper reaction layer of the fracture samples may be due to the more porous physical structure of the natural fracture surfaces. In general, the porosity of their interfacial region is approximately one order of magnitude larger than for the artificially ruptured samples. The source of ferrous iron is predominantly biotite in the mica gneisses, and both hornblende and biotite in the tonalite sample.

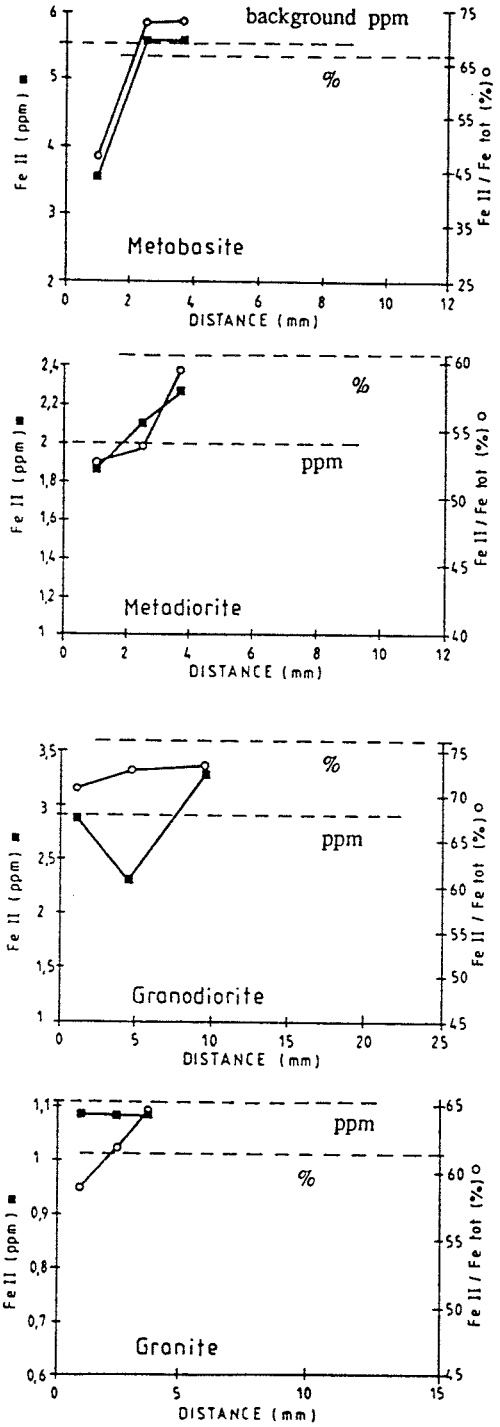

Remarks:

a) -average background Fe II 5.5 % w
-porosity 0.06 % v
-lightly banded
-fresh, lightly altered

b) -average background Fe II 2.0 % w
-porosity 0.09 % v
-foliated
-altered

c) -average background Fe II 2.9 % w
-porosity 0.08 % v
-foliated
-altered
-hornblende heteroneneously distributed

d) -average background Fe II 1.1 % w
-porosity 0.18 % v
-lightly foliated
-fresh, lighly altered

Figure 3. Profiles of artificially ruptured a) metabasite, b) metadiorite, c) granodiorite I and d) granite.

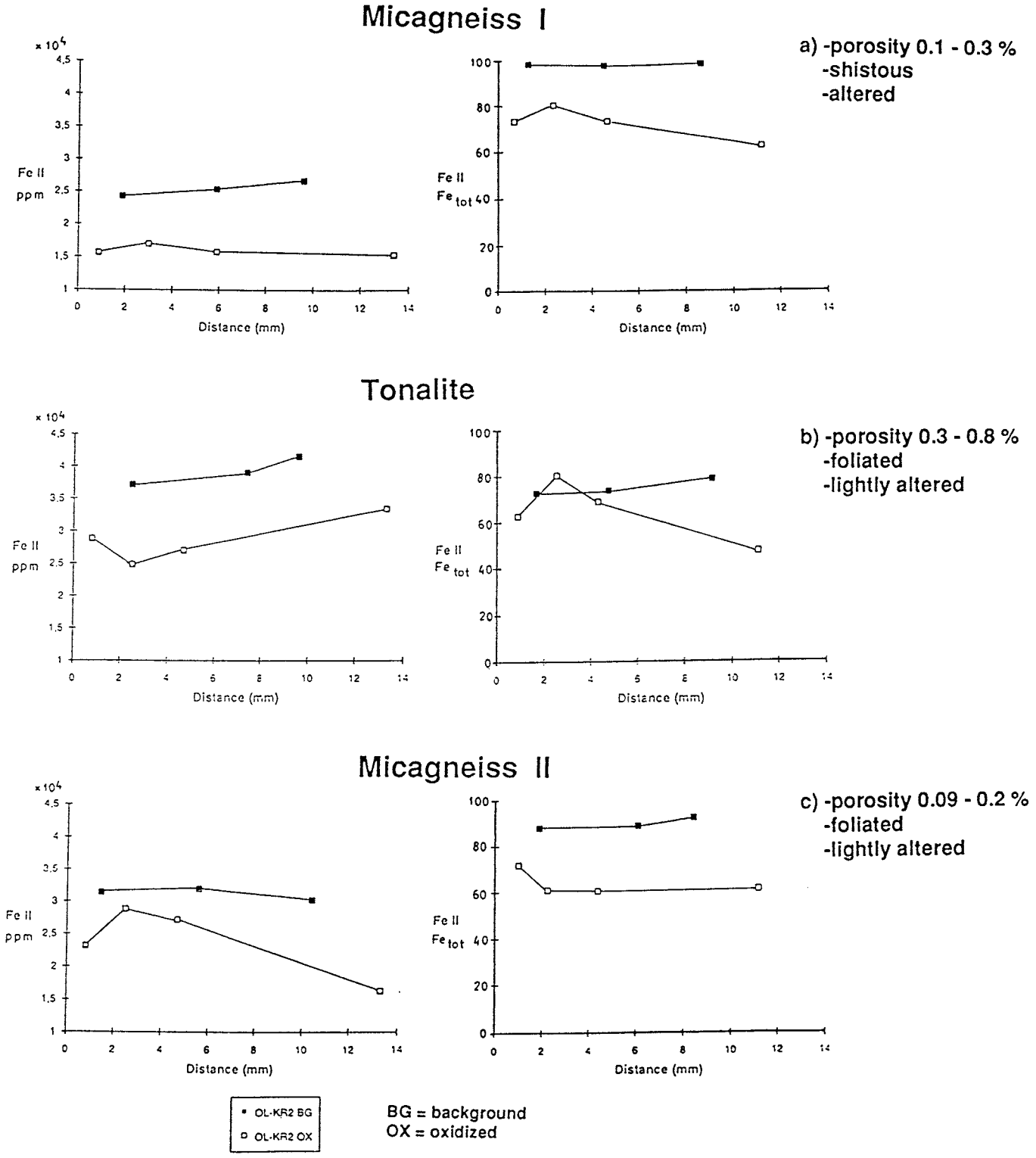

Figure 4. Natural fracture profiles.

The analytical results are compiled in Table 4 along with the relevant sample location (the middle point of the sample), reaction time, FeII and Fe_{tot} contents, and $FeII/Fe_{tot}$ ratios.

Uncertainty in the analysed values cannot be statistically determined in this experiment. Reproducibility of the FeII content has been tested by comparing different analysis methods with each other before starting the experiments. The adopted volumetric method has the best resolution of the methods available for FeII analyses (accuracy is maintained down to 1.0 ppm, WILSON 1960). Replicate analyses for the standard samples yield a maximum standard deviation of 0.03 % of the mean (PIRHONEN et al.1990a).

Sample/rock type	Sample index	Remarks/Distance of middle point from surface	Fe II *10⁴ppm	Fe_{tot} *10⁴ppm	$Fe(II)/Fe_{tot}$ %
Rock powder	Fi8-1/0I	background	2.92	3.72	78.5
Granodiorite I	/0II	"	2.88	3.67	78.5
	$/0_2$	amb.cond, 3 weeks	2.46	3.44	72.5
	$/0_2$	100 bar , 4 weeks	2.63	3.68	71.5
	$/0_2$	" , 7 weeks	2.58	3.63	71.1
	$/0_2$	, 12 weeks	2.63	3.71	70.9
Granodiorite II	Fi8-2/0	background (-90)	2.58	2.83	67.4
	/0	" (-91)	2.34 (-10 %)	2.98 (-20 %)	78.5
	/air	in air , 32 weeks	2.04 (-20 %)	-	-
	$/0_2$I	amb.cond, 9 weeks	1.61	2.77	60.7
Whole rock					
Granodiorite I	Fi8-1/1.1 CR	1 mm, 3 weeks	3.63	5.01	72.5
	/1.2 CR	4,5 mm, "	3.13	4.25	73.6
	/1.3 CR	9,5 mm, "	2.55	3.49	73.1
	/2.2 CR	1.0 mm, 6 weeks	2.98	4.07	73.2
	/2.2 CR	4.5 mm,	3.07	4.10	73.3
	/2.3 CR	9.5 mm,	3.04	4.16	73.1
	/3.1 CR	1 mm, 10 weeks	2.90	4.08	71.1
	/3.2 CR	4.5 mm,	2.32	3.18	73.0
	/3.3 CR	9.5 mm,	3.29	4.47	73.6
Granodiorite II	Fi8-1/1 P0	0.5 mm, 12 weeks	1.77	2.99	59.2
	/2 P0	1.7 mm,	1.75	2.90	60.3
	/3 P0	2.9 mm,	1.71	2.83	60.4
	/4 P0	10.8 mm,	2.01	3.69	54.5
	/5 P0	21.0 mm,	1.81	3.23	56.0
	/6 P0				
	/7 P0				
Metadiorite	Kas02-1/0	background	1.89	3.12	60.6
	/air	in air , 32 weeks	1.75 (-7.5 %)	-	-
	/1 PO	0.5 mm, 12 weeks	1.94	4.22	46.0
	/2 PO	1.7 mm, "	2.26	4.25	53.2
	/3 PO	2.9 mm, "	2.09	4.15	50.4
	/6 PO	10.8 mm, "	1.11	2.71	41.1
	/7 PO				
	Kas02-1/1 CR	1.0 mm, "	1.86	3.51	52.9
	/2 CR	2.5 mm, "	2.10	3.89	54.0
	/3 CR	3.7 mm, "	2.26	3.79	59.6
Granite	Kas02-2/0	background	1.11	1.81	61.3
	/air	in air , 32 weeks	0.89 (-20 %)	-	-
	/1 P0	0.5 mm, 12 weeks	0.89	1.84	48.4
	/2 P0	1.7 mm, "	0.85	1.71	49.7
	/3 P0	2.9 mm, "	0.69	1.31	52.7
	/6 P0	10.8 mm, "	0.73	1.45	50.3
	/7 P0				
	Kas02-2/1 CR	1.0 mm,	1.09	1.84	59.2
	/2 CR	2.5 mm,	1.05	1.69	62.1
	/3 CR	3.7 mm,	1.03	1.59	64.8
Metabasite	Fi4/0	background	5.51	8.39	65.7
	/air	in air , 32 weeks	2.83 (-49 %)	-	-
	/1 PO	0.5 mm, 12 weeks	2.35	8.11	29.0
	/2 PO	1.7 mm,	3.06	8.44	36.3
	/3 PO	2.9 mm,	2.43	8.37	29.9
	/6 PO	10.8 mm,	2.94	7.22	40.7
	/7 PO				
	Fi4/1 CR	1.0 mm,	3.53	7.30	48.4
	/2 CR	2.5 mm,	5.53	7.61	72.7
	/3 CR	3.7 mm,	5.52	7.56	73.0
Micagneiss I	OLKR2/0-1 FR	background, 1.9 mm	2.43	2.51	96.8
	/0-2 FR	" , 5.9 mm	2.54	2.70	95.2
	/0-3 FR	" , 9.6 mm	2.66	2.80	95.0
	$/0_2$-1 FR	100 bar/12 weeks,0.9 mm	1.57	2.15	73.0
	$/0_2$-2 FR	" ,3.0 mm	1.70	2.15	79.0
	$/0_2$-3 FR	" ,5.9 mm	1.58	2.18	72.5
	$/0_2$-6 FR	" ,13.4 mm	1.54	2.54	60.6
Tonalite	SYKR3/0-1 FR	background, 1.5 mm	3.15	4.01	78.6
	/0-2 FR	" , 5.6 mm	3.19	4.06	78.6
	/0-3 FR	" , 10.4 mm	3.02	3.72	81.2
	$/0_2$-1 FR	100 bar/12 weeks,0.8 mm	2.32	3.51	66.1
	$/0_2$-2 FR	" ,2.5 mm	2.88	3.49	82.5
	$/0_2$-3 FR	" ,4.7 mm	2.71	3.68	73.6
	$/0_2$-6 FR	" ,13.3 mm	1.63	3.31	49.2
MicagneissII	SYKR5/0-1 FR	background, 2.5 mm	3.71	4.16	89.2
	/0-2 FR	" , 7.4 mm	3.89	4.35	89.4
	/0-3 FR	" , 9.6 mm	4.15	4.46	93.0
	$/0_2$-1 FR	100 bar/12 weeks,0.8 mm	2.88	3.97	72.5
	$/0_2$-2 FR	" ,2.5 mm	2.49	4.23	58.9
	$/0_2$-3 FR	" ,4.7 mm	2.71	4.60	58.9
	$/0_2$-6 FR	,13.3 mm	3.34	5.62	59.4
Mineral powder					
	biotite/0	background	14.29	17.51	81.6
	$/0_2$	100 bar/12 weeks	7.99	16.66	48.0
	hypersthene/0		9.67	10.59	91.3
	$/0_2$I		8.96	10.11	88.6
	$/0_2$II		7.06	9.47	74.6
	hornblende/0		4.97	8.78	56.6
	$/0_2$		4.55	8.59	53.0
	olivine/0		4.92	5.47	89.9
	$/0_2$		3.92	5.39	72.7

Table 4. Iron in rock and minerals before (background) and after oxidation experiments. Fe II and Fe_{tot} have been analyzed with volumetric and atomic adsorption (AAS) methods respectively except pyrite and magnrtite that have been analysed with Mössbauer spectrosc. The mean deviation of the volumetric method is 0.01-0.03 (Pirhonen 1990).

3.2 Calculated redox capacity of rock

The redox capacity of the solid rock samples are presented in Table 5. The decrease of Fe II is averaged over the whole profile, except the last analyses point if it goes beyond the background. For example, Kas 02-2 (CR): background 1.11 $ppm \cdot 10^4$

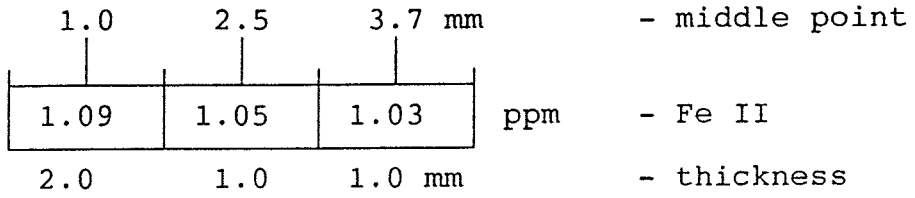

$$\text{Average contents} = \frac{2.0 \cdot 1.09 + 1.0 \cdot 1.05 + 1.0 \cdot 1.03}{4.0} = 1.065$$

and decrease of FeII = 1.11 - 1.06 = 0.045 ppm,
i.e. Δ 4.0 %

The average decrease of iron II varied from 2 % to 36 % in ruptured (CR) rock samples. In natural fracture samples, the variation was from 18 % to 39 %. The redox capacity calculated from the decrease of Fe II ranged from about 18 to 620 mol_{FeII}/m^3 and 320 to 580 mol_{FeII}/m^3 for the ruptured and the natural fracture samples, respectively.

In the polished samples, that are not included in the results (Appendix 8), the decrease of Fe II was about 10 % more than in the ruptured rock samples. The polished samples might have been affected by the heat introduced during the mechanical polishing procedure, although, no porosity increase was observed in the microscopy studies.

Table 5. The redox capacity of the rock. Calculated from the decrease of Fe II averaged over the profile. The last analyses point (Table 4) has not been taken into account if it goes beyond the background.

Ruptured (CR) samples	Porosity %	Density 10^3 kg/m^3	Initial Fe II 10^4 ppm	Decrease of Fe II %	Redox capacity (Fe II)
1. Metadiorite with fds-meca-crysts (Kas 02-1)	0.09	2.7	1.89	2	0,4 g/kg i.e. 18 mol/m^3
2. Granite (Kas 02-2)	0.18	2.6	1.11	4	0.6 g/kg 1.e. 28 mol/m^3
3. Granodio-rite (Fi 8-1)	0.06	2.7	2.92	15	4.4 g/kg i.e. 211 mol/m^3
4. Metabasite (Fi 4)	0.08	2.9	5.51	36	12.0 g/kg i.e. 620 mol/m^3
Fracture samples					
1. Mica gneiss, no filling (SY-KR5)	0.52	2.6	3.83	18	6.9 g/kg i.e. 320 mol/m^3
2. Tonalite mica gneiss, carbonate (OL-KR2)	0.20	2.7	2.55	38.5	9.8 g/kg i.e. 473 mol/m^3
3. Tonalite, slickenside (SY-KR2)	0.15	2.7	3.10	39	12.1 g/kg i.e. 580 mol/m^3

4. CONCLUSIONS

This study has shown that the redox capacity of the crystalline rocks can be measured with the test arrangement used, even though uncertainties in the analysed values cannot be statistically determined in this experiment. The results indicate that solid rock clearly has a measurable reducing ability due to oxidation of Fe(II) in rock. The oxidized fracture samples have much more extensive reaction layer than the artificially ruptured rock samples. The measured redox capasity of all the rock samples vary from 18 to 620 mol_{FeII}/m^3 as the porosities of the samples range between 0.06 and 0.52 %, and FeII contents between 1.11 and 5.51 % w.

LIST OF REFERENCES

Dryar, B.M., Naney, M.T. and Swanson, S.E. (1987). Effects of quench methods on Fe^{3+}/Fe^{+2} rations A Mössbauer and wetchemical study, Am. Mineralogist, Vol. 72, 792-800.

Pirhonen, V., Pitkänen, P., Takala, J. and Arilahti, E. (1990a). Design and preliminary results of redox capacity. Mat. Res. Soc. Symp. Proc. Vol 212, 839-847.

Pirhonen, V., Pitkänen, P. and Front, K. (1990b). Diffusion interfaces of fractures in granitic rocks. Nuclear Waste Commission of Finnish Power Companies, report YJT-10-90, 19 p. + app. 21 p.

White, A.F. and Yee, A. (1985). Aqueous oxidation-reduction kinetics associated with coupled electron-cation transfer from iron-containing silicates at 25 ^{o}C, Geochim. Cosmochim. Acta Vol. 49, pp. 1263-1275.

Wikman, H., Kornfält, K-A., Riad, L., Munier, R. (1988). Detailed investigation of the drillcores KAS 02, KAS 03 and KAS 04 on Äspö island and KLX 01 at Laxemar. SKB Progress Report 25-88-11, 59 p.

Wilson, A.D. (1960). The micro-determination of ferrous iron in silicate minerals by a volumetric and a colorimetric method. Analyst 85, 823-827.

Determination of ferrous and total iron of rock powder

To avoid undesirable oxidation during preparation of samples, all preliminary work was done in an inert atmosphere. For the same reason samples were decomposed in the presence of quinquivalent vanadium. Added vanadium acted as a "Fe-calendar" according to reaction

$$Fe^{2+} + V^{5+} = Fe^{3+} + V^{4+}$$

in which equilibrium is dependent on (H^+) so that by adjusting the pH, the original Fe(II)/Fe(III) was able to be restored.

PROCEDURE

The amount of sample weighed was from 75 mg up to 500 mg, depending on the ferrous iron content of rocks analyzed. Samples were placed in approx. 50 ml polypropylene containers. After addition of 8 ml NH_4VO_3 and 10 ml 40 % HF samples were shaken overnight in a laboratory shaker. As suitable decomposing time was found to be more than 16 hours but less than 40 hours, otherwise uncontrolled oxidation cannot be avoided. Decomposing was followed by an addition of 6,0 g of solid H_3BO_3, immediate cooling of containers and stirring with a magnetic stirrer for at least 1 hour, surrounded by cold water. The addition of boric acid was necessary to release metals from their fluorides and to protect glassware against the attack of HF. Samples were diluted to 50 ml and centrifuged remove excess boric acid and insoluble CaF_2 precipitates.

Determination of ferrous iron by spectrophotometry

Four dilutions were made to cover the pH-range from pH 5,55 to 6,10, each containing 250 µl, 500 µl, 750 µl or 1000 µl

of centrifuged sample, 9,5 ml DIP solution and diluted to 50 ml with deionisized water. At higher pH, the Fe(III)-acetate complex causes background errors and at lower pH, redox equilibrium was not quantitative on the Fe(II) side. It was found that the optimum pH was not same for all samples, and was also slightly different for samples with remarkably different mineral composition and thus pH-scanning was necessary.

Standards were made of a suitable amount of Fe(III) standard solution, 200 µl HXL, 360 µl matrix solution and 1,9 ml of DIP in each standard, even in bland, covering concentrations from 0 ppm to 5 ppm. Standards were made daily to avoid problems caused by their instability.

The absorptions were measured at a wavelength of 521 nm.

Determination of total iron by atomic absorption spectrophotometry

Centrifuged solutions were diluted to a 10 times larger volume.

Standards were made from suitable amounts of Fe(III) standard solution, 5,0 ml saturated H_3BO_3 solution, 0,8 ml NH_4VO_3 stock solution and 1,0 ml 40 % HF, covering concentrations from 0 ppm to 30 ppm. Standards were stable enough for storage.

The absorptions were measured at a wavelength of 372 nm.

STOCK SOLUTIONS

NH_4VO_3	8,13 g solid NH_4VO_3, 100 ml 10 N H_2SO_4, dilution to 500 ml
DIP	50 ml 0,15 % 2'2-bipyridin solution, 60 g solid NH_4Ac, dilution to 250 ml

HXL	10 % hydroxylammoniumchloride solution
Matrix	2 ml 40 % HF, 20 ml H_3BO_3 and 1,6 ml NH_4VO_3 stock solution, no dilution

CONCLUSIONS

Ferrous iron determination procedure is a routine analysis, which does not give absolute accuracy, but it does provide satisfactory precision, especially when comparing samples with the same or almost the same mineral composition. The main error source is the background effect caused by the Fe(III)-acetate complex. The disturbing effect of possible redox potentials in addition to than Fe/V seems to be negligible, but it needs further examination.

Sample and thin section photographs

Appendix 2.1

OL-KR2, fracture sample

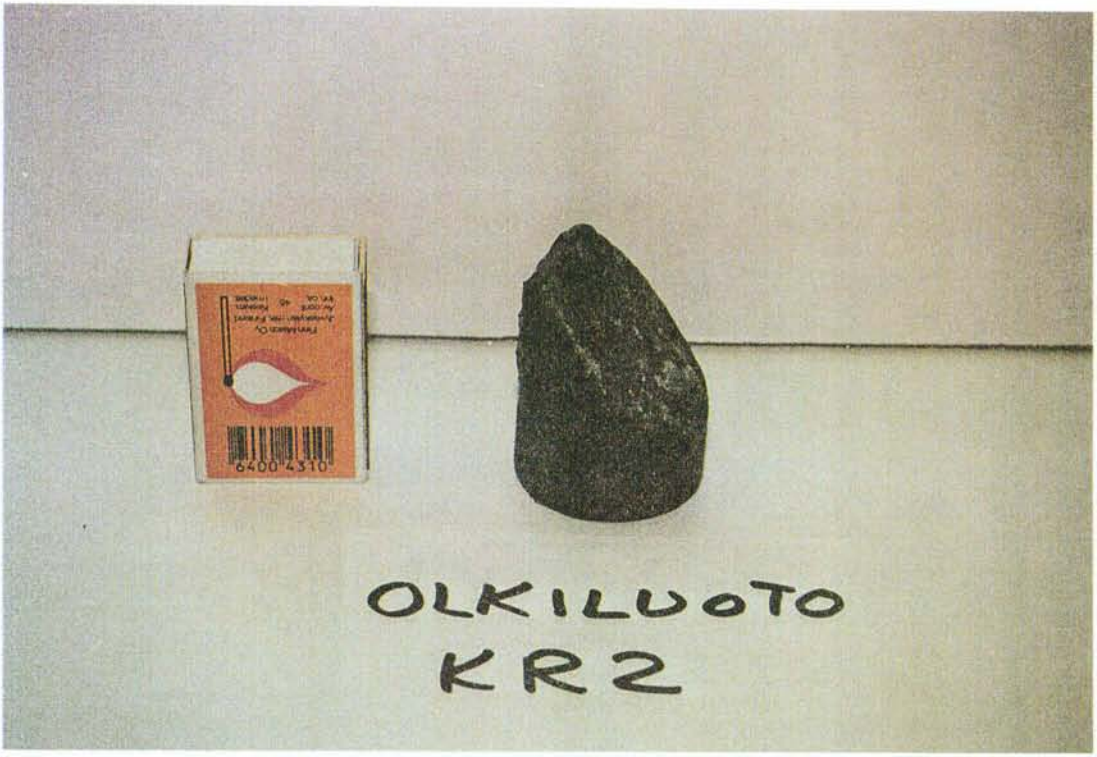

Appendix 2.2

SY-KR3, fracture sample

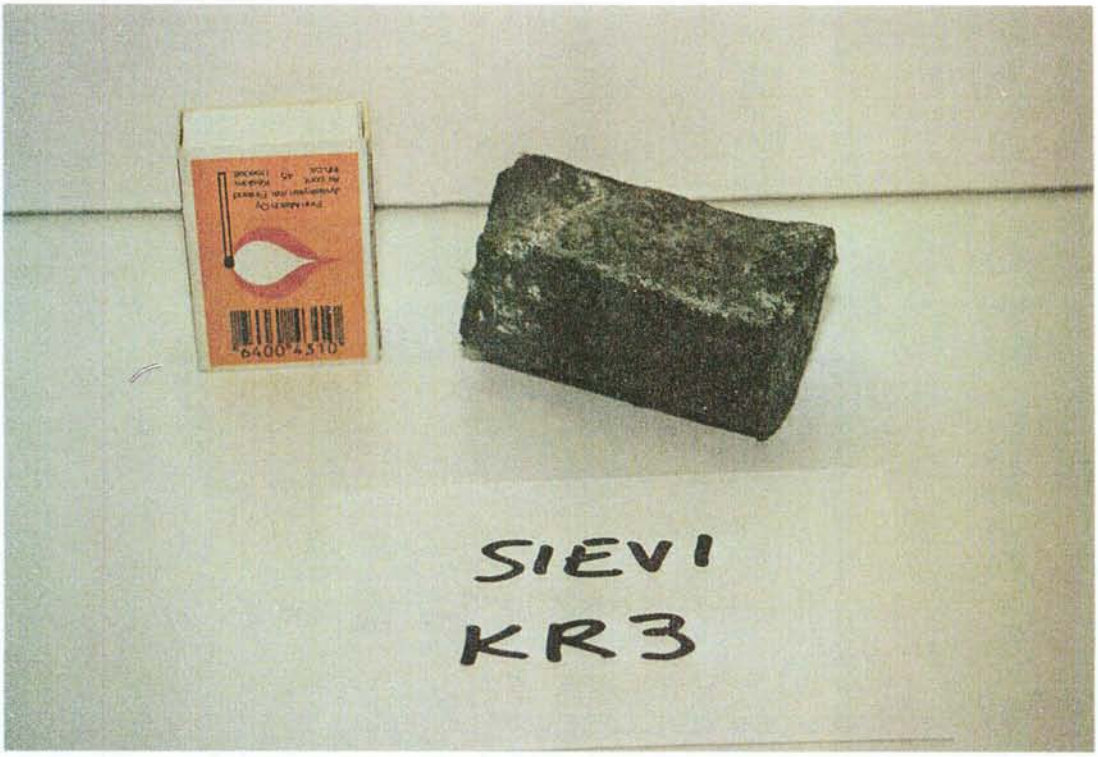

Appendix 2.3

SY-KR5, fracture sample

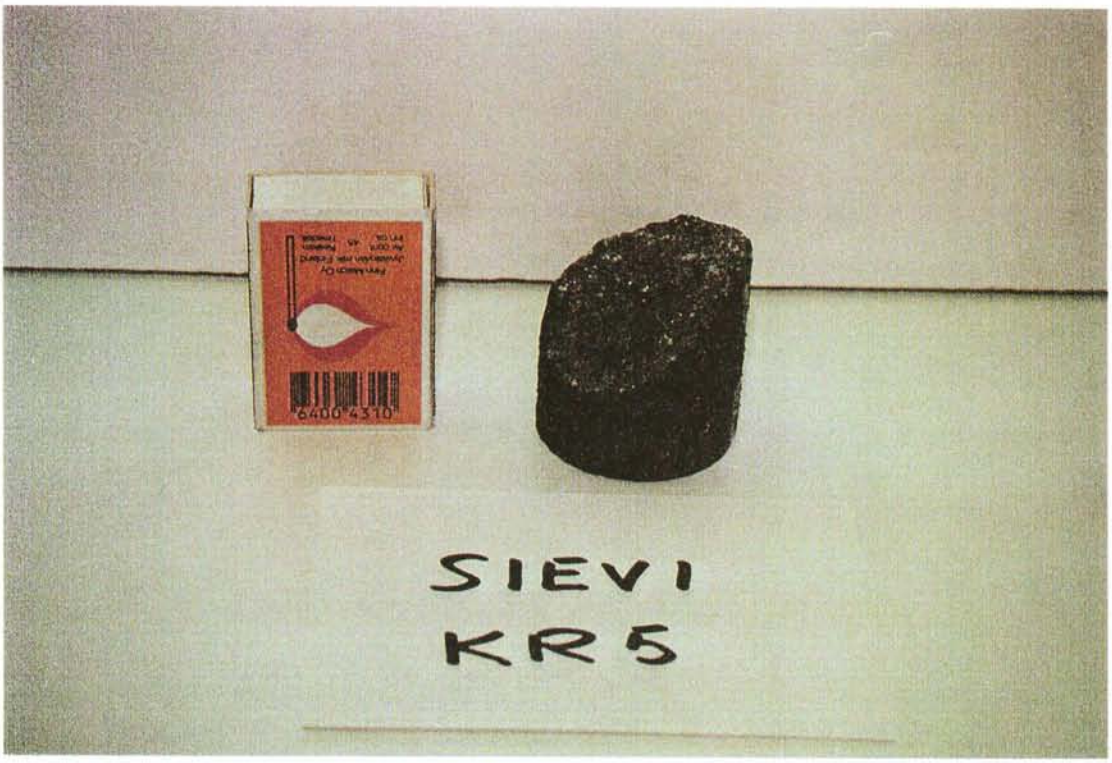

Appendix 2.4

Kas 02-1, crack (left) and polished (right) samples

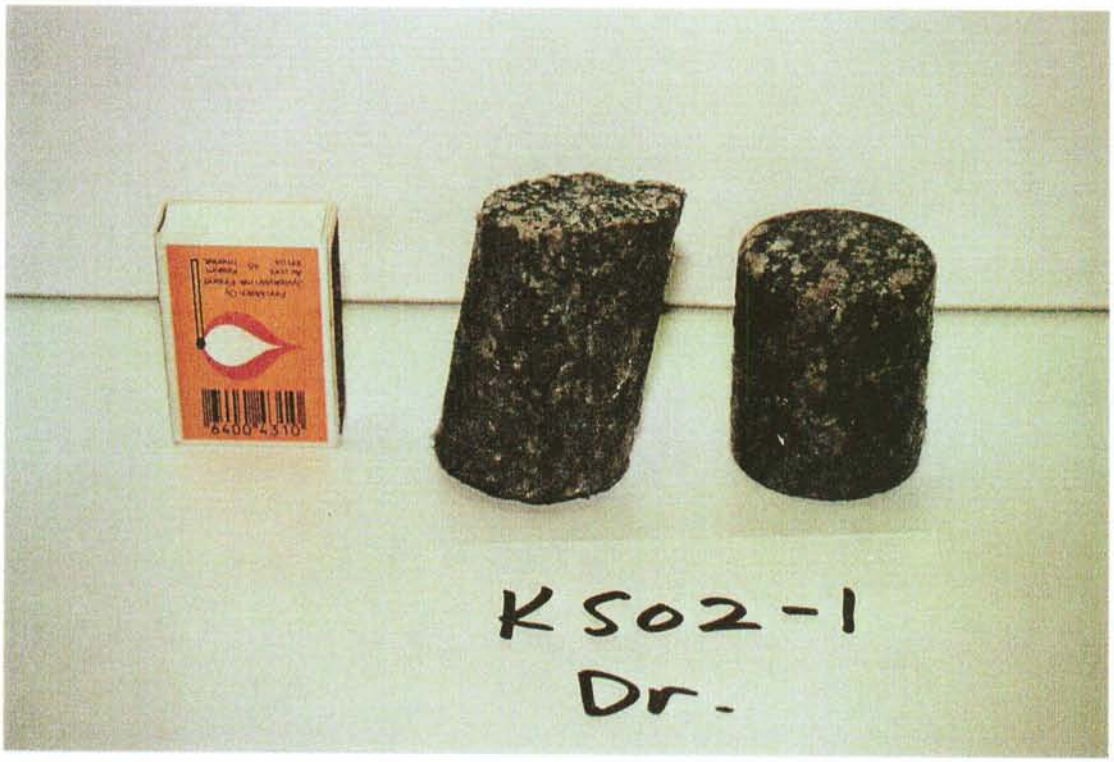

Appendix 2.5

Kas 02-2, crack (left) and polished (right) samples

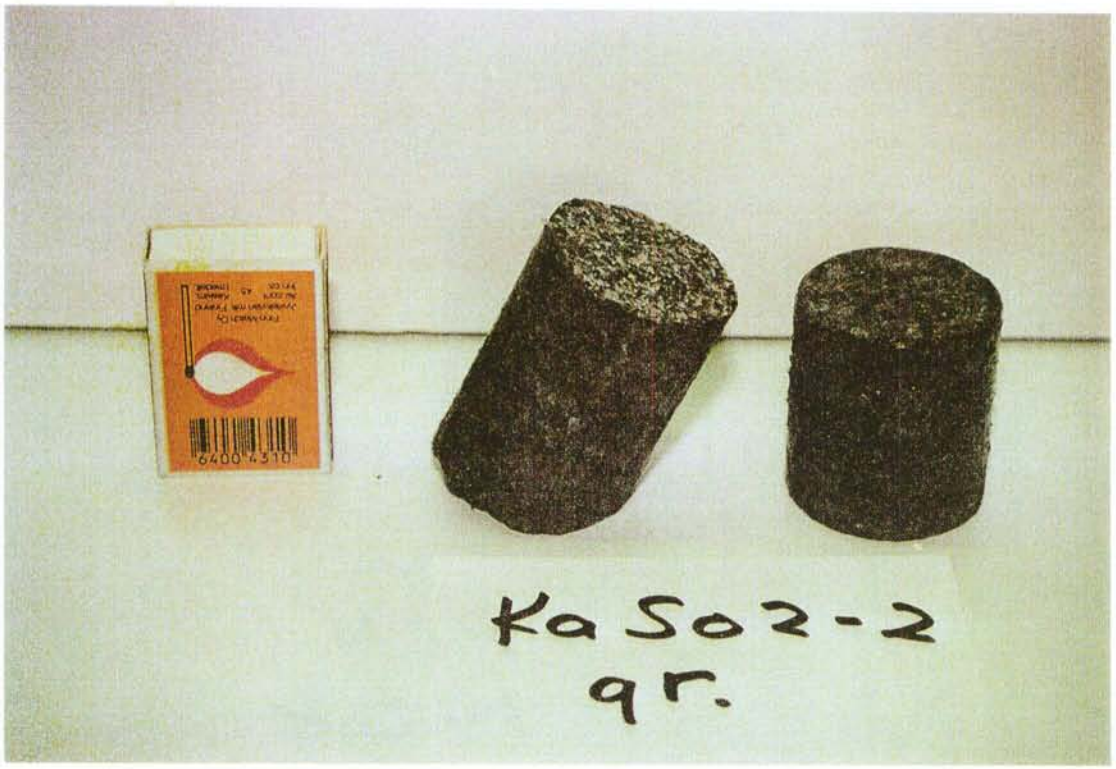

Appendix 2.6

Fi8, crack (left) and polished (right) samples

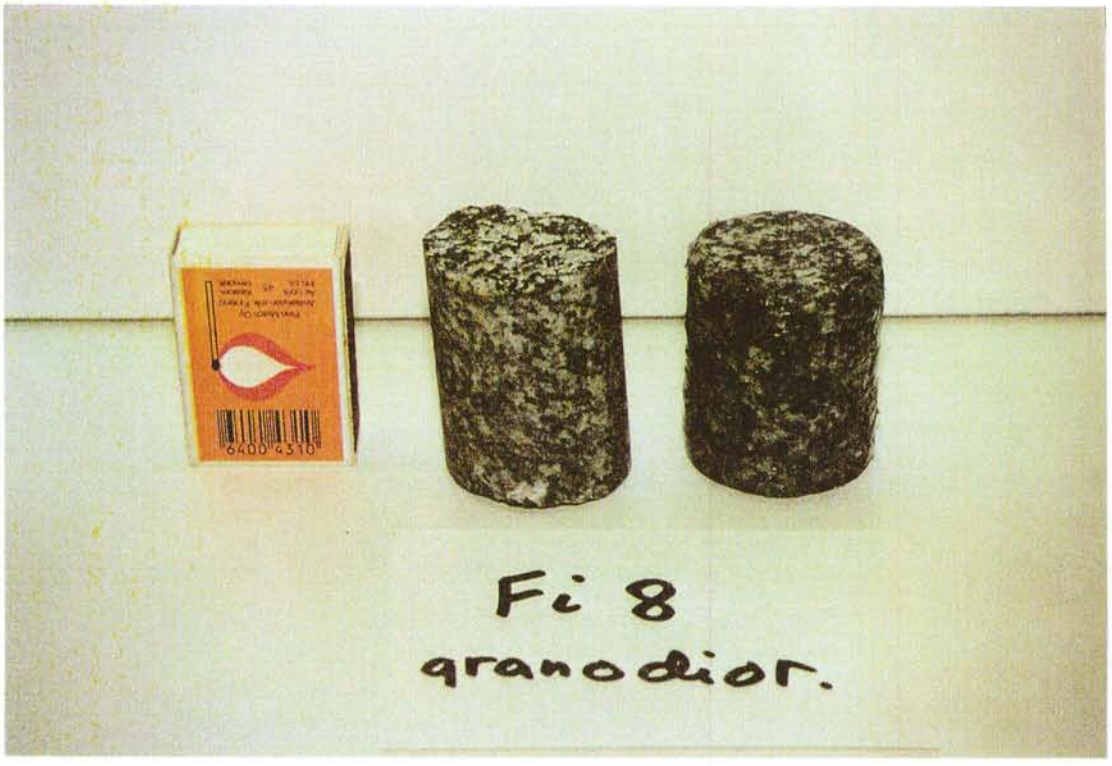

Appendix 2.7

Fi4, crack (left) and polished (right) samples

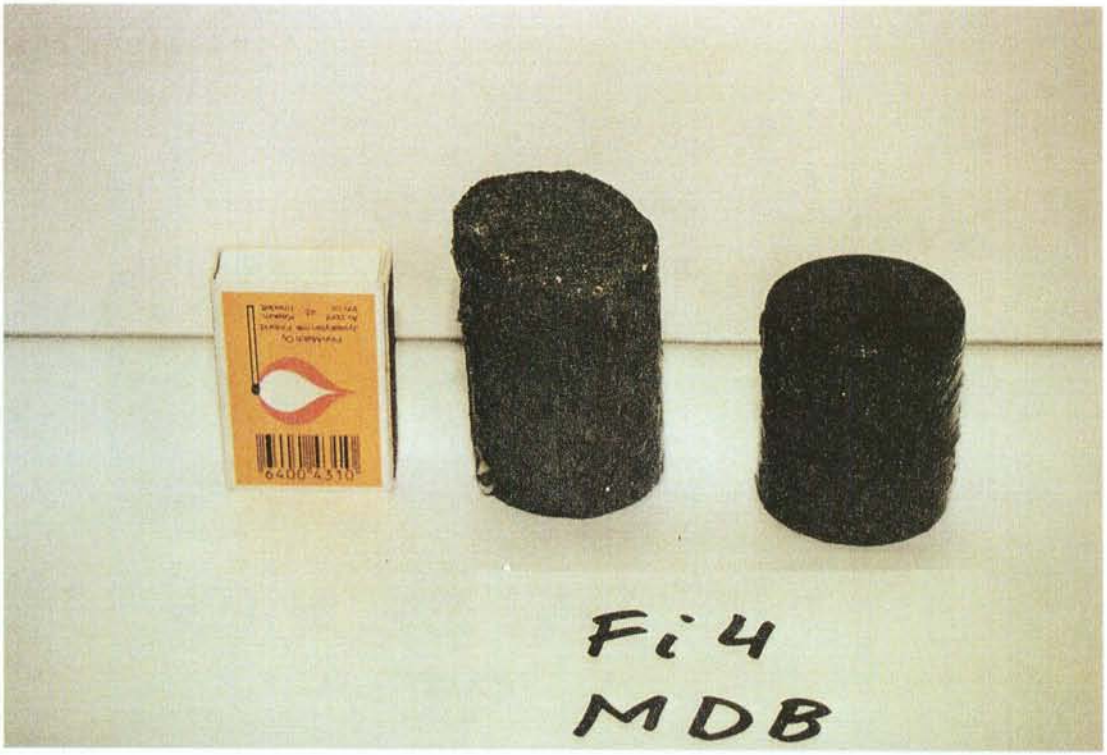

Appendix 2.8

OL-KR2, main fracture surface (x10)

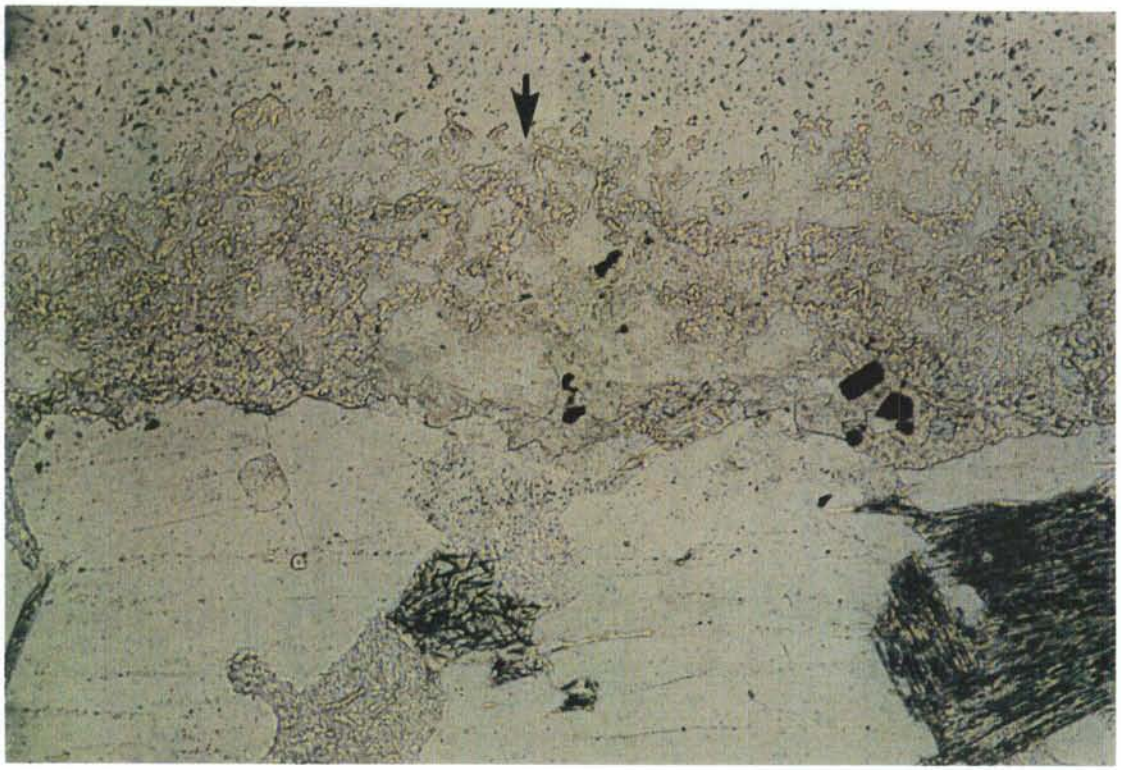

Appendix 2.9

OL-KR2, diffusion chanels from carbonate filled midsample fracture (x20)

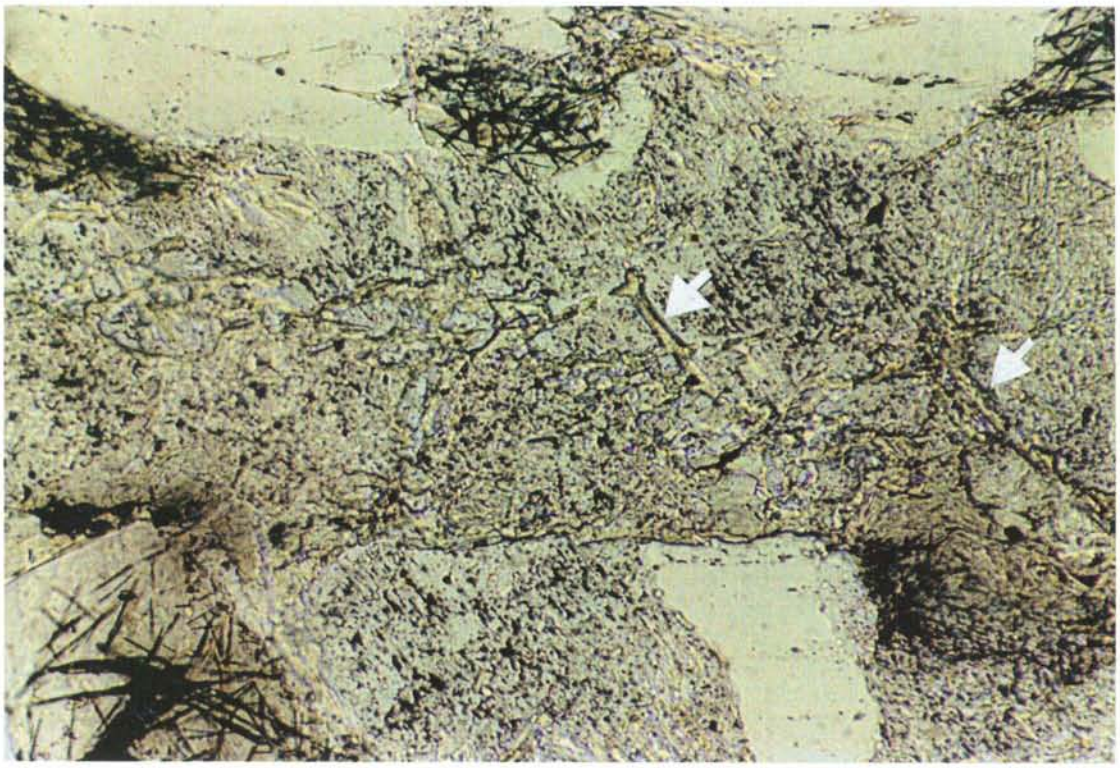

Appendix 2.10

OL-KR2, fluid inclusion rims in quartz (x40)

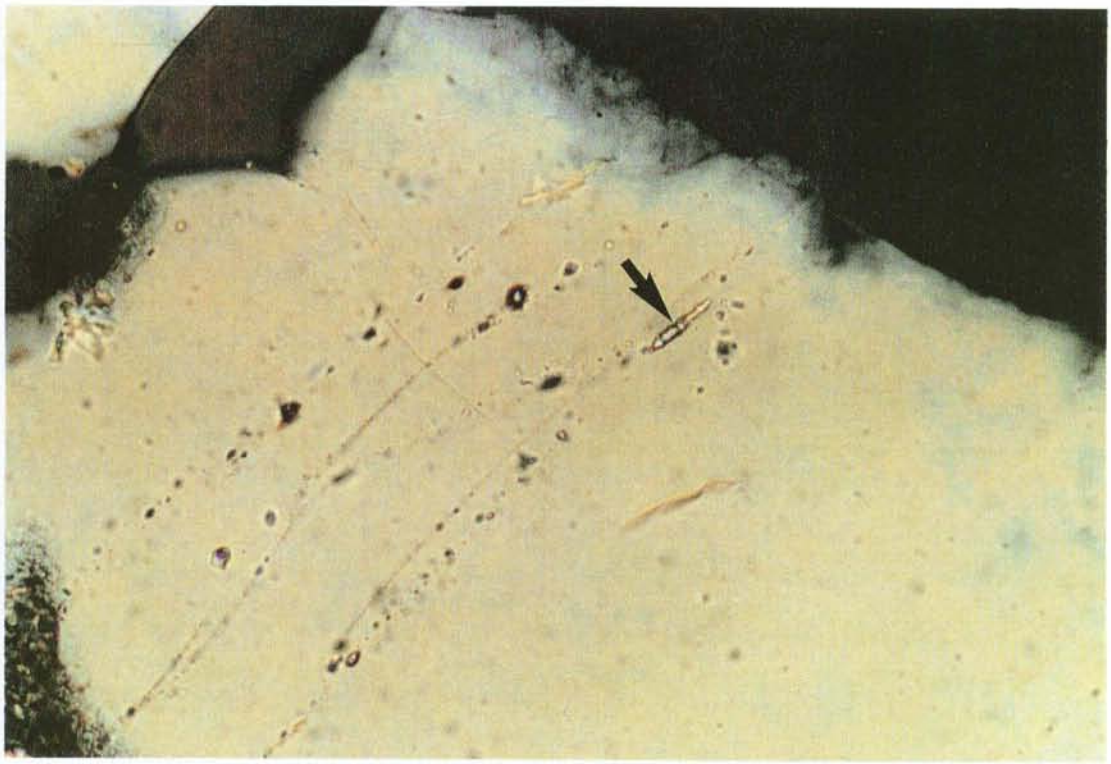

Appendix 2.11

SY-KR3, altered biotite (?) on fracture surface (x10)

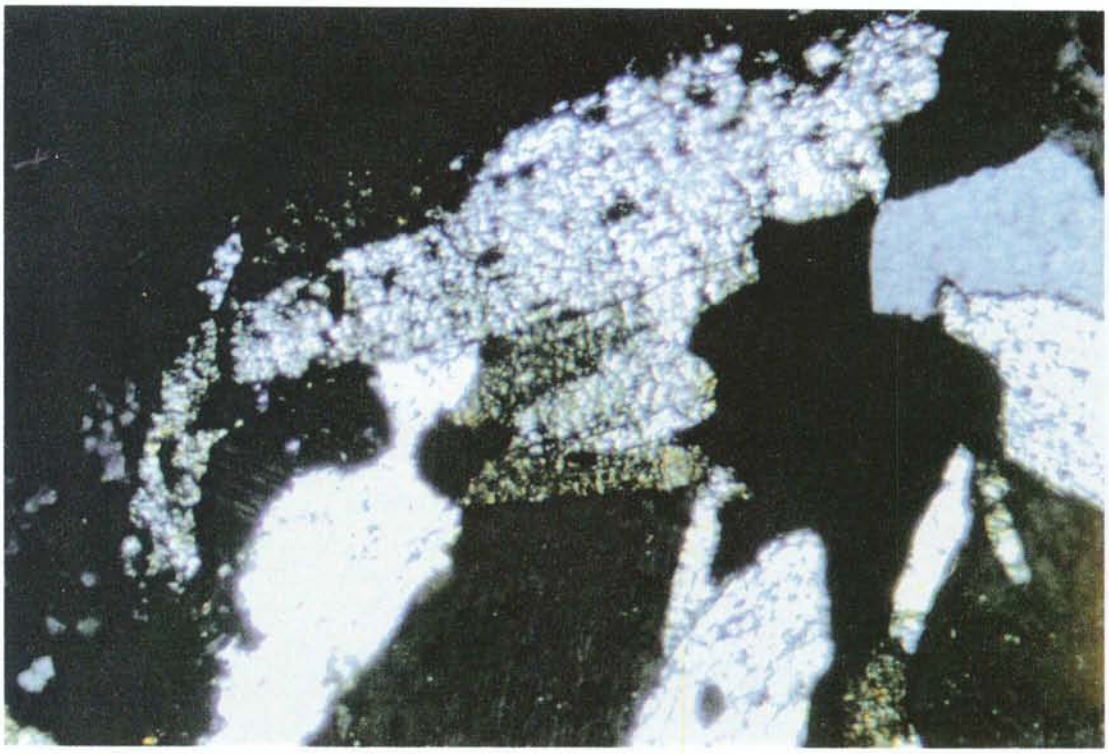

Appendix 2.12

SY-KR5, fluid inclusion rims in quartz (x20)

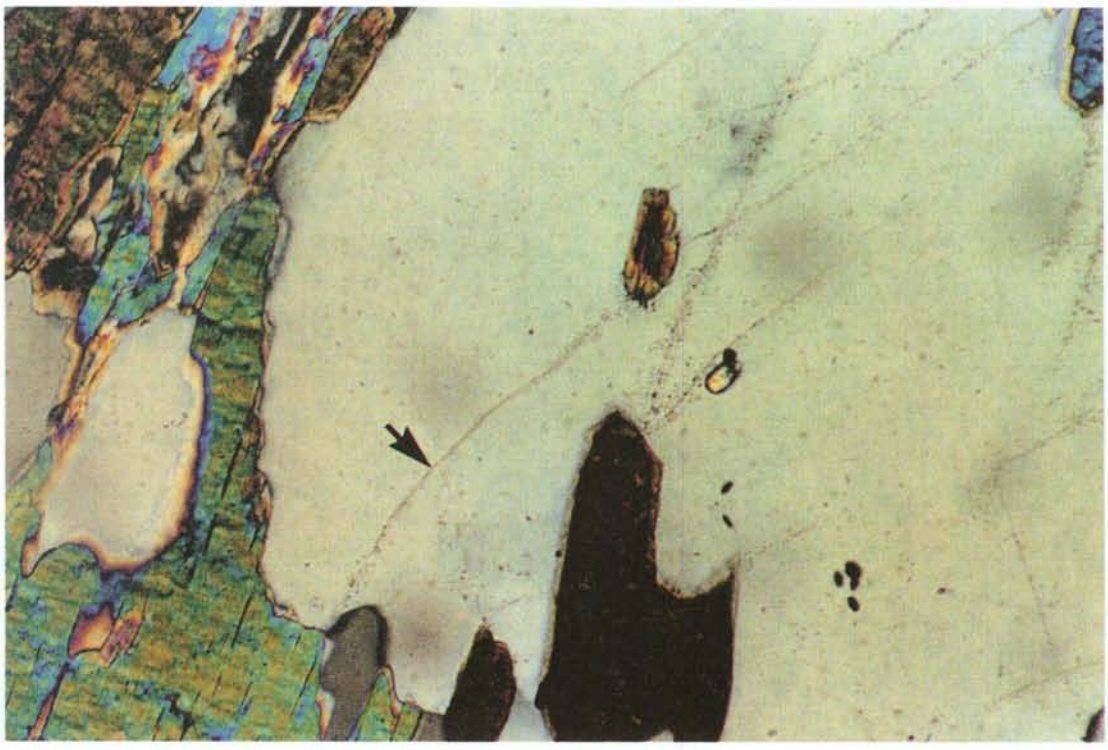

Appendix 2.13

SY-KR5, carbonate filled fractures (x10)

Appendix 2.14

Kas 02-1, elongated fracture in quartz and plagioclase (x10)

Appendix 2.15

Fi8-1, microfractures in quartz (x20)

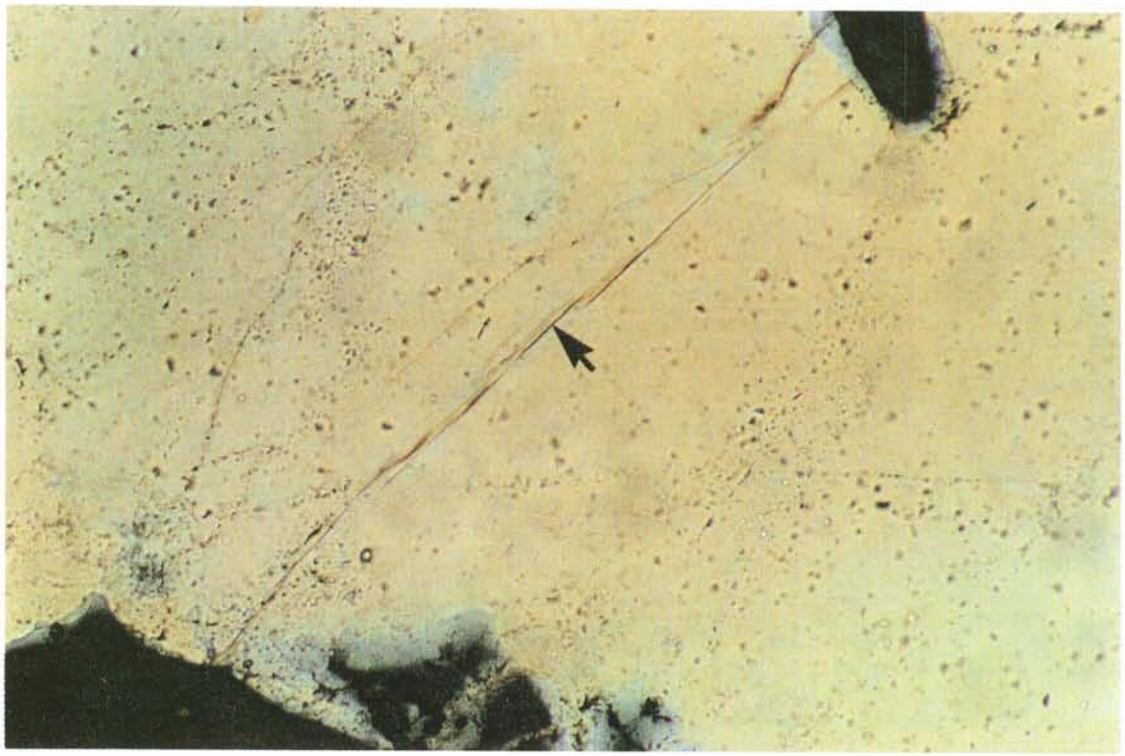

Appendix 2.16

Intensive fracturing in hypersthene (x4)

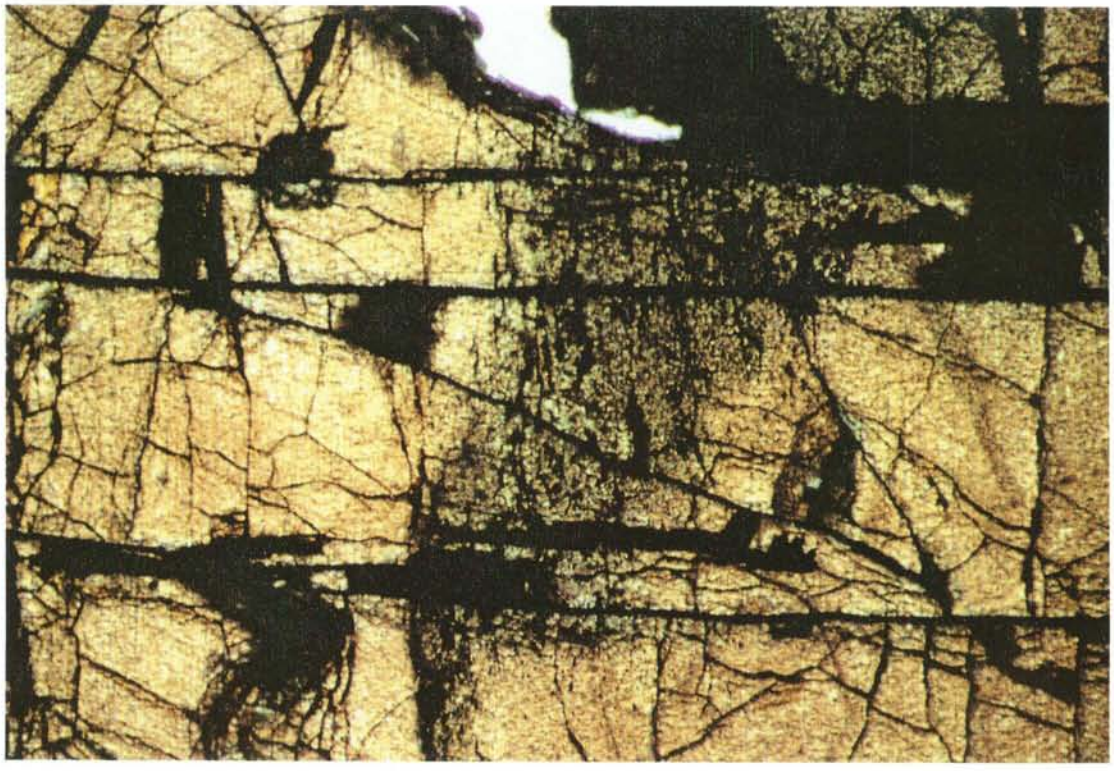

Porosity profiles of fracture samples

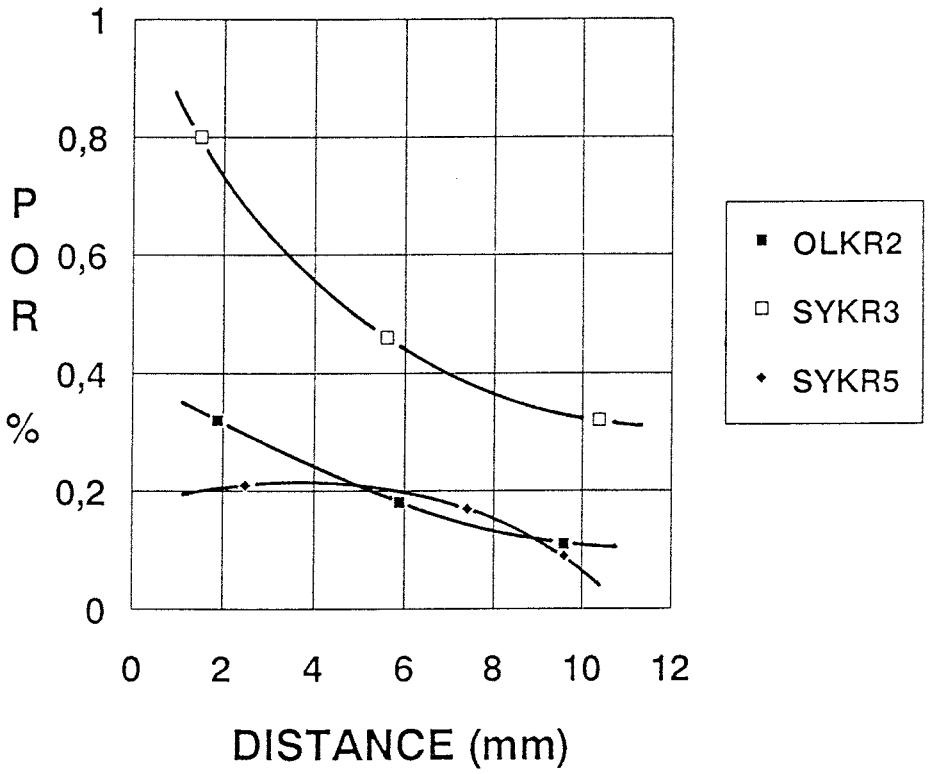

Chemical contents of synthetic granite water

ALLARD WATER

Ca	18 mg/l
Mg	4.3 mg/l
Na	52.5 mg/l
K	3.9 mg/l
SiO_2	12 mg/l
Cl	70 mg/l
HCO_3	123 mg/l
SO_4	9.6 mg/l
pH	8.0 - 8.2
ionic strength	0.0045

Oxygen contents of granite water with time in test run

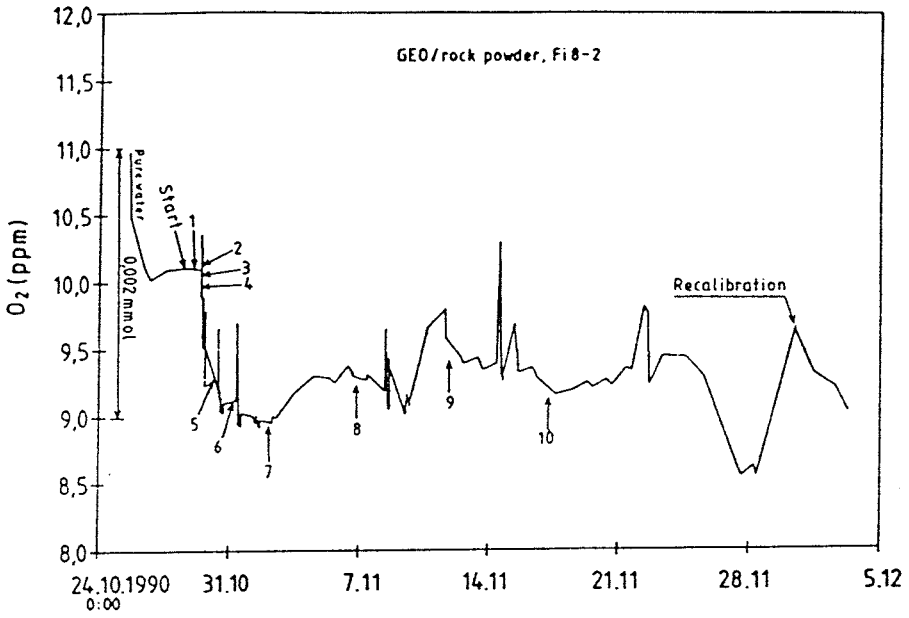

Cation contents of granite water with time in test run

CATION ANALYSES

VTT/GEO (GEO 91431)	0-sample	1-sample	2-sample	3-sample	4-sample	5-sample
Veijo Pirhonen	29.10.90 klo 9.45	29.10.90 klo 10.15	29.10.90 klo 12.10	29.10.90 klo 13.50	29.10.90 klo 16.00	30.10.90 klo 9.50
KATIONIT CATIONS						
Kalsium (Ca) mg/l	17	16	16	16	16	16
Magnesium (Mg) mg/l	4.2	4.3	4.2	4.2	4.3	4.3
Natrium (Na) mg/l	52	51	54	53	54	51
Kalium (K) mg/l	1.2	3.6	1.9	2.0	2.3	4.2
Aluminium (Al) mg/l	< 0.05	0.09	0.08	0.09	0.10	0.17
Rauta (Fe) mg/l	< 0.05	0.17	< 0.05	< 0.05	0.06	0.30
Piidioksidi (SiO_2) mg/l	7.9	7.9	8.0	8.0	7.9	7.8
ANIONIT ANIONS						
Fluoridi (F^-) mg/l	5.0	4.3	4.4	4.8	5.2	5.2
Kloridi (Cl^-) mg/l	31	54	34	51	39	34
Fosfaatti (PO_4^{3-}) mg/l	< 1.5	< 1.5	< 1.5	< 1.5	< 1.5	< 1.5
Sulfaatti (SO_4^{2-}) mg/l	12	11	11	12	11	11

Samples stabilized by concentrated HNO_3 except samples 7 and 8.

CATION ANALYSES (ICP)

VTT/GEO (GEO 91431)	6-sample	7-sample	8-sample			
Veijo Pirhonen	31.10.90 klo 9.50	8.11.90 klo 9.45	22.11.90 klo 13.40			
KATIONIT CATIONS						
Kalsium (Ca) mg/l	16	14	14			
Magnesium (Mg) mg/l	4.3	4.2	4.3			
Natrium (Na) mg/l	53	49	53			
Kalium (K) mg/l	3.6	10	11			
Aluminium (Al) mg/l	0.14	0.12	0.07			
Rauta (Fe) mg/l	0.11	0.21	< 0.05			
Piidioksidi (SiO_2) mg/l	7.9	7.7	5.2			
ANIONIT ANIONS						
Fluoridi (F^-) mg/l	4.3	< 1	< 1			
Kloridi (Cl^-) mg/l	36	35	47			
Fosfaatti (PO_4^{3-}) mg/l	< 1.5	< 1.5	< 1.5			
Sulfaatti (SO_4^{2-}) mg/l	12	11	5.2			

Samples stabilized by concentrated HNO_3 except samples 7 and 8.

a)

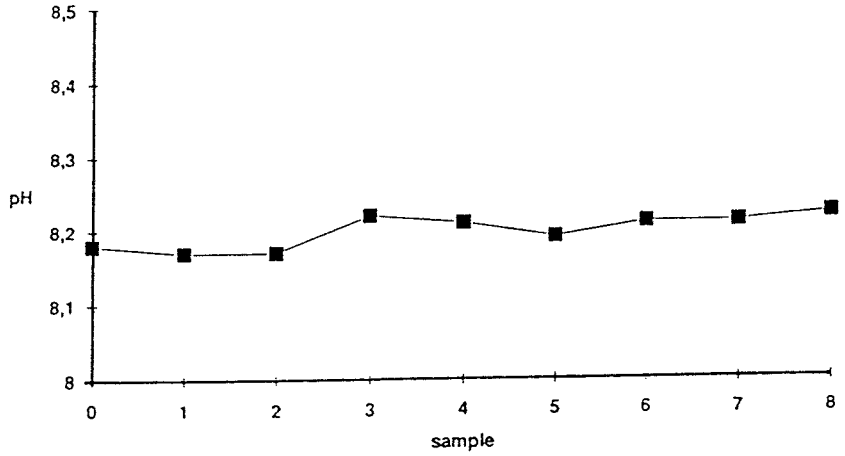
8,5
8,4
8,3
pH
8,2
8,1
8
0
1
2
3
4
5
6
7
8
sample

b)

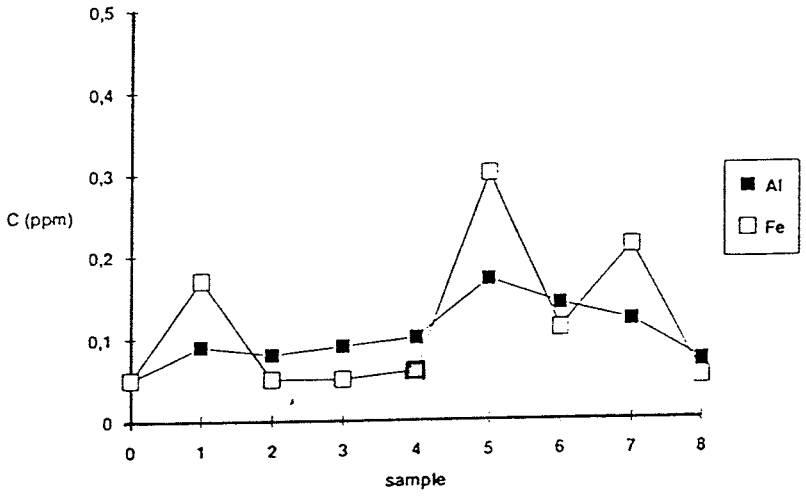
0,5
0,4
0,3
C (ppm)
0,2
0,1
0
0
1
2
3
4
5
6
7
8
sample
Al
Fe

Species in solution

c)

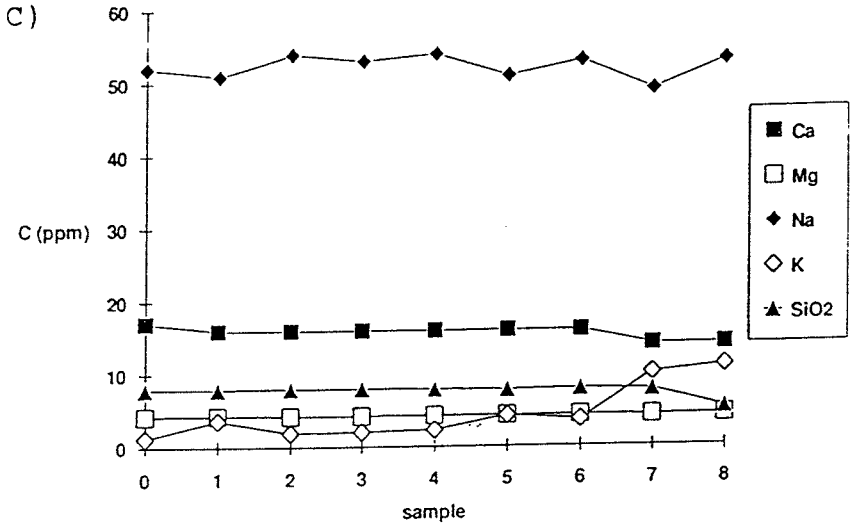

d)

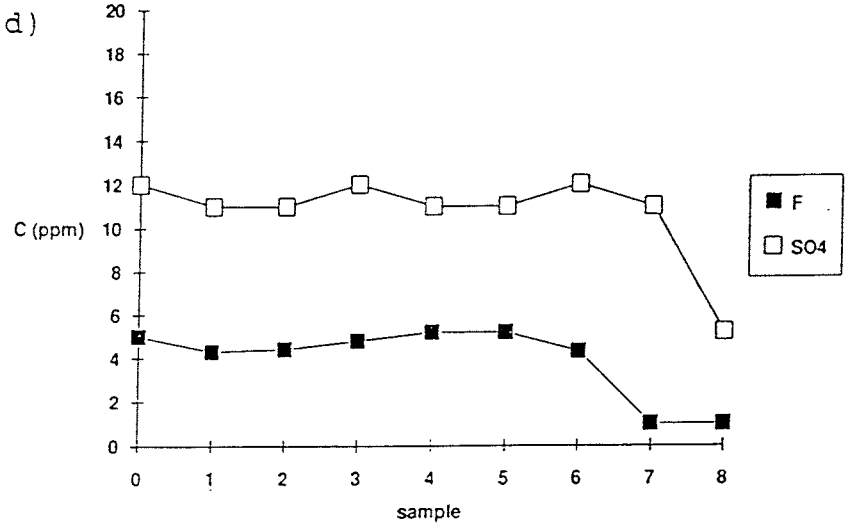

e)

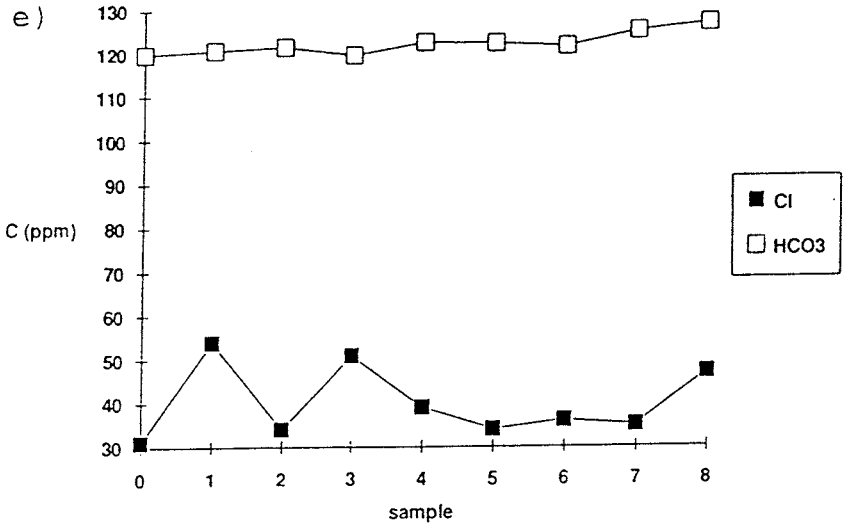

Mössbauer diagrams of pyrite and magnetite

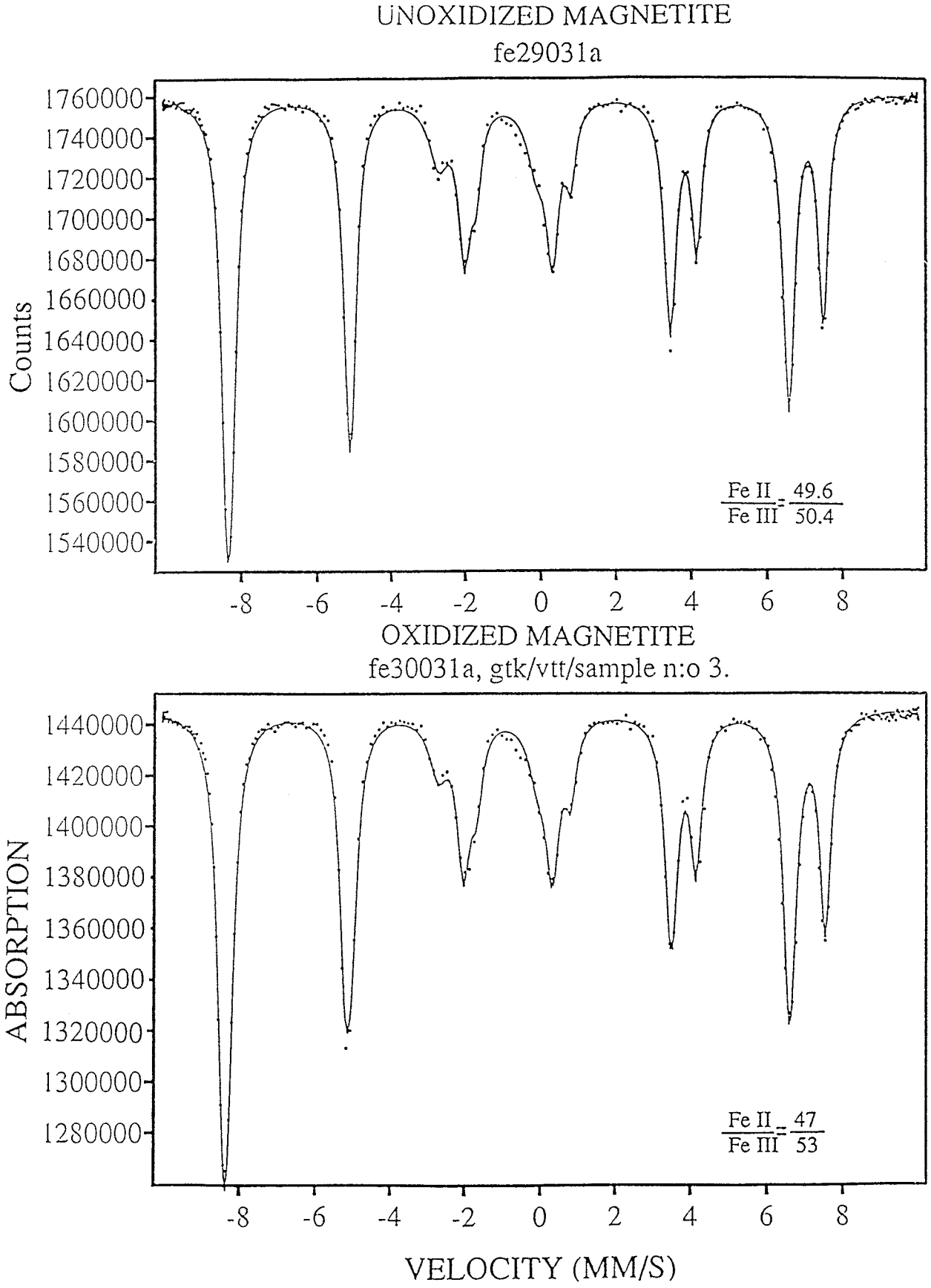

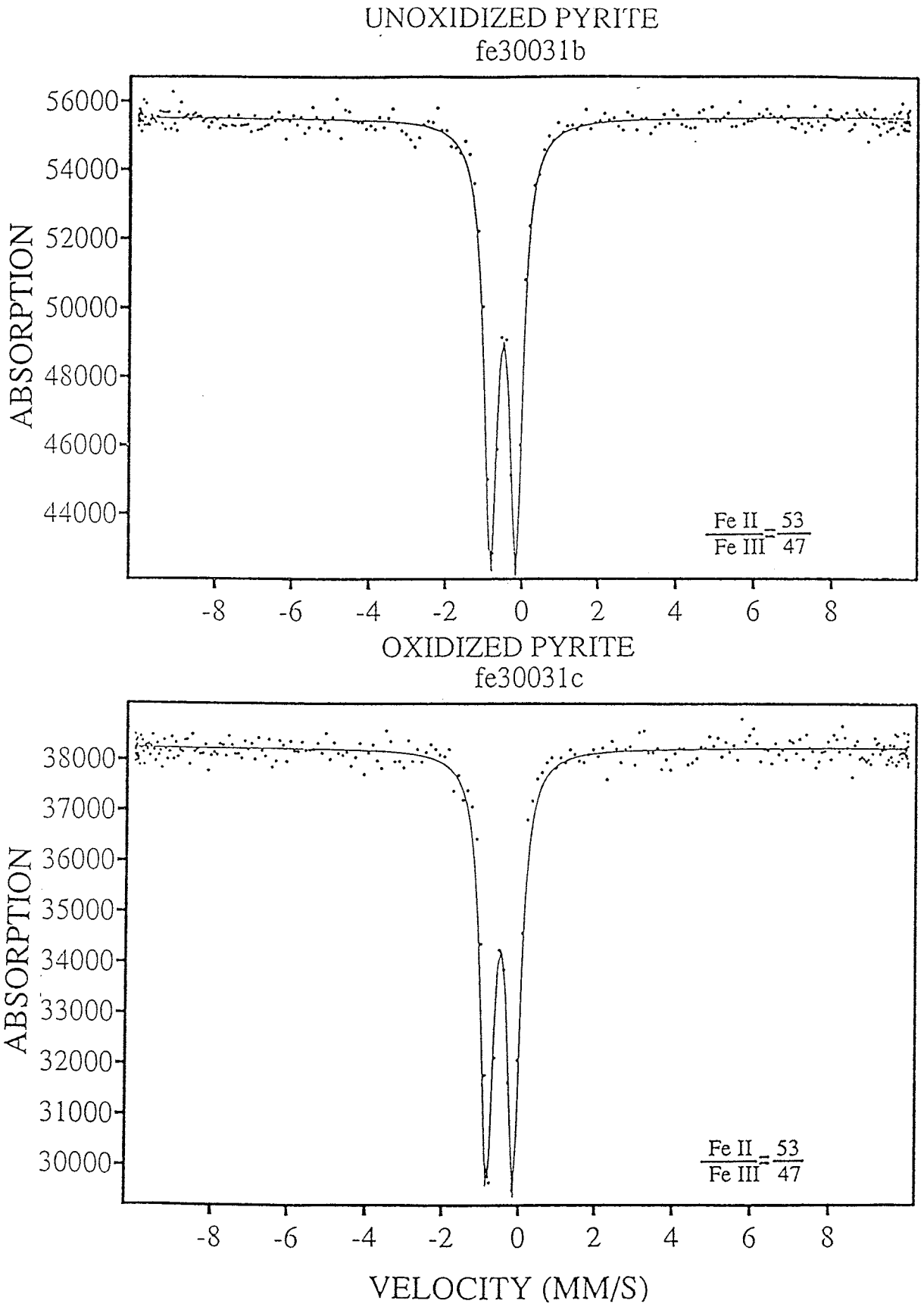
UNOXIDIZED PYRITE
fe30031b
ABSORPTION
56000
54000
52000
50000
48000
46000
44000
Fe II / Fe III = 53 / 47
-8 -6 -4 -2 0 2 4 6 8
OXIDIZED PYRITE
fe30031c
ABSORPTION
38000
37000
36000
35000
34000
33000
32000
31000
30000
Fe II / Fe III = 53 / 47
-8 -6 -4 -2 0 2 4 6 8
VELOCITY (MM/S)

Fe II profiles of polished rock samples

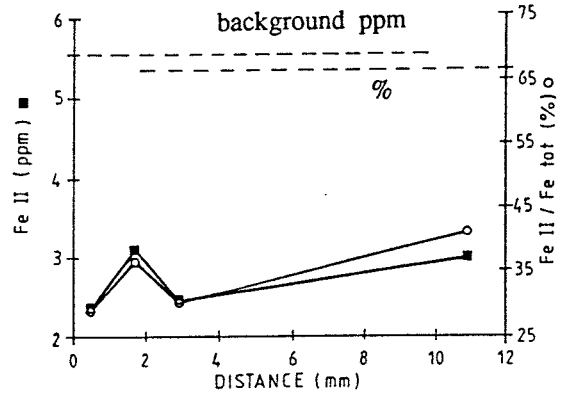

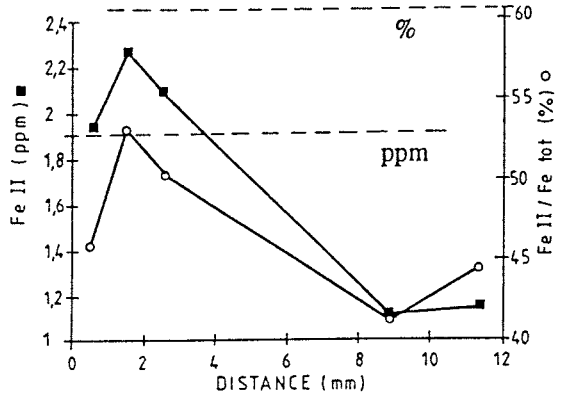

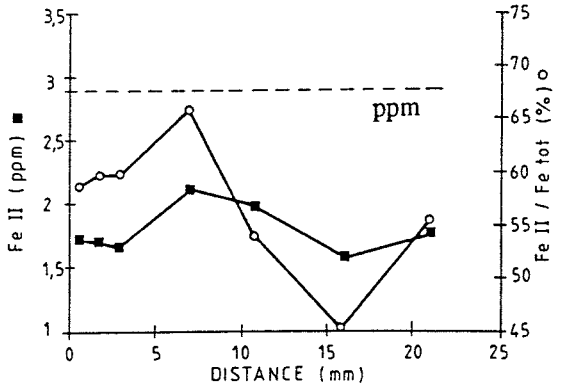

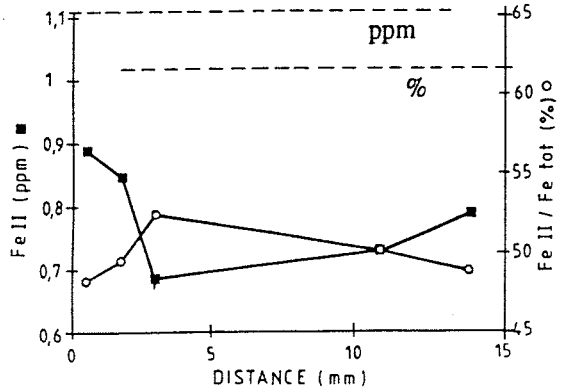

List of SKB reports

Annual Reports

1977-78
TR 121
KBS Technical Reports 1 – 120
Summaries
Stockholm, May 1979

1979
TR 79-28
The KBS Annual Report 1979
KBS Technical Reports 79-01 – 79-27
Summaries
Stockholm, March 1980

1980
TR 80-26
The KBS Annual Report 1980
KBS Technical Reports 80-01 – 80-25
Summaries
Stockholm, March 1981

1981
TR 81-17
The KBS Annual Report 1981
KBS Technical Reports 81-01 – 81-16
Summaries
Stockholm, April 1982

1982
TR 82-28
The KBS Annual Report 1982
KBS Technical Reports 82-01 – 82-27
Summaries
Stockholm, July 1983

1983
TR 83-77
The KBS Annual Report 1983
KBS Technical Reports 83-01 – 83-76
Summaries
Stockholm, June 1984

1984
TR 85-01
Annual Research and Development Report 1984
Including Summaries of Technical Reports Issued during 1984. (Technical Reports 84-01 – 84-19)
Stockholm, June 1985

1985
TR 85-20
Annual Research and Development Report 1985
Including Summaries of Technical Reports Issued during 1985. (Technical Reports 85-01 – 85-19)
Stockholm, May 1986

1986
TR 86-31
SKB Annual Report 1986
Including Summaries of Technical Reports Issued during 1986
Stockholm, May 1987

1987
TR 87-33
SKB Annual Report 1987
Including Summaries of Technical Reports Issued during 1987
Stockholm, May 1988

1988
TR 88-32
SKB Annual Report 1988
Including Summaries of Technical Reports Issued during 1988
Stockholm, May 1989

1989
TR 89-40
SKB Annual Report 1989
Including Summaries of Technical Reports Issued during 1989
Stockholm, May 1990

1990
TR 90-46
SKB Annual Report 1990
Including Summaries of Technical Reports Issued during 1990
Stockholm, May 1991

Technical Reports

List of SKB Technical Reports 1991

TR 91-01
Description of geological data in SKB's database GEOTAB
Version 2
Stefan Sehlstedt, Tomas Stark
SGAB, Luleå
January 1991

TR 91-02
Description of geophysical data in SKB database GEOTAB
Version 2
Stefan Sehlstedt
SGAB, Luleå
January 1991

TR 91-03
1. The application of PIE techniques to the study of the corrosion of spent oxide fuel in deep-rock ground waters
2. Spent fuel degradation
R S Forsyth
Studsvik Nuclear
January 1991

TR 91-04
Plutonium solubilities
I Puigdomènech[1], J Bruno[2]
[1]Enviromental Services, Studsvik Nuclear, Nyköping, Sweden
[2]MBT Tecnologia Ambiental, CENT, Cerdanyola, Spain
February 1991

TR 91-05
Description of tracer data in the SKB database GEOTAB
SGAB, Luleå
April, 1991

TR 91-06
Description of background data in the SKB database GEOTAB
Version 2
Ebbe Eriksson, Stefan Sehlstedt
SGAB, Luleå
March 1991

TR 91-07
Description of hydrogeological data in the SKB's database GEOTAB
Version 2
Margareta Gerlach (ed.)
Mark Radon Miljö MRM Konsult AB, Luleå
December 1991

TR 91-08
Overview of geologic and geohydrologic conditions at the Finnsjön site and its surroundings
Kaj Ahlbom[1], Sven Tirén[2]
[1]Conterra AB
[2]Sveriges Geologiska AB
January 1991

TR 91-09
Long term sampling and measuring program. Joint report for 1987, 1988 and 1989. Within the project: Fallout studies in the Gideå and Finnsjö areas after the Chernobyl accident in 1986
Thomas Ittner
SGAB, Uppsala
December 1990

TR 91-10
Sealing of rock joints by induced calcite precipitation. A case study from Bergeforsen hydro power plant
Eva Hakami[1], Anders Ekstav[2], Ulf Qvarfort[2]
[1]Vattenfall HydroPower AB
[2]Golder Geosystem AB
January 1991

TR 91-11
Impact from the disturbed zone on nuclide migration – a radioactive waste repository study
Akke Bengtsson[1], Bertil Grundfelt[1], Anders Markström[1], Anders Rasmuson[2]
[1]KEMAKTA Konsult AB
[2]Chalmers Institute of Technology
January 1991

TR 91-12
Numerical groundwater flow calculations at the Finnsjön site
Björn Lindbom, Anders Boghammar, Hans Lindberg, Jan Bjelkås
KEMAKTA Consultants Co, Stockholm
February 1991

TR 91-13
Discrete fracture modelling of the Finnsjön rock mass
Phase 1 feasibility study
J E Geier, C-L Axelsson
Golder Geosystem AB, Uppsala
March 1991

TR 91-14
Channel widths
Kai Palmqvist, Marianne Lindström
BERGAB-Berggeologiska Undersökningar AB
February 1991

TR 91-15
Uraninite alteration in an oxidizing environment and its relevance to the disposal of spent nuclear fuel
Robert Finch, Rodney Ewing
Department of Geology, University of New Mexico
December 1990

TR 91-16
Porosity, sorption and diffusivity data compiled for the SKB 91 study
Fredrik Brandberg, Kristina Skagius
Kemakta Consultants Co, Stockholm
April 1991

TR 91-17
Seismically deformed sediments in the Lansjärv area, Northern Sweden
Robert Lagerbäck
May 1991

TR 91-18
Numerical inversion of Laplace transforms using integration and convergence acceleration
Sven-Åke Gustafson
Rogaland University, Stavanger, Norway
May 1991

TR 91-19
NEAR21 - A near field radionuclide migration code for use with the PROPER package
Sven Norman[1], Nils Kjellbert[2]
[1]Starprog AB
[2]SKB AB
April 1991

TR 91-20
Äspö Hard Rock Laboratory. Overview of the investigations 1986-1990
R Stanfors, M Erlström, I Markström
June 1991

TR 91-21
Äspö Hard Rock Laboratory. Field investigation methodology and instruments used in the pre-investigation phase, 1986-1990
K-E Almén, O Zellman
June 1991

TR 91-22
Äspö Hard Rock Laboratory. Evaluation and conceptual modelling based on the pre-investigations 1986-1990
P Wikberg, G Gustafson, I Rhén, R Stanfors
June 1991

TR 91-23
Äspö Hard Rock Laboratory. Predictions prior to excavation and the process of their validation
Gunnar Gustafson, Magnus Liedholm, Ingvar Rhén, Roy Stanfors, Peter Wikberg
June 1991

TR 91-24
Hydrogeological conditions in the Finnsjön area. Compilation of data and conceptual model
Jan-Erik Andersson, Rune Nordqvist, Göran Nyberg, John Smellie, Sven Tirén
February 1991

TR 91-25
The role of the disturbed rock zone in radioactive waste repository safety and performance assessment. A topical discussion and international overview.
Anders Winberg
June 1991

TR 91-26
Testing of parameter averaging techniques for far-field migration calculations using FARF31 with varying velocity.
Akke Bengtsson[1], Anders Boghammar[1], Bertil Grundfelt[1], Anders Rasmuson[2]
[1]KEMAKTA Consultants Co
[2]Chalmers Institute of Technology

TR 91-27
Verification of HYDRASTAR. A code for stochastic continuum simulation of groundwater flow
Sven Norman
Starprog AB
July 1991

TR 91-28
Radionuclide content in surface and groundwater transformed into breakthrough curves. A Chernobyl fallout study in an forested area in Northern Sweden
Thomas Ittner, Erik Gustafsson, Rune Nordqvist
SGAB, Uppsala
June 1991

TR 91-29
Soil map, area and volume calculations in Orrmyrberget catchment basin at Gideå, Northern Sweden
Thomas Ittner, P-T Tammela, Erik Gustafsson
SGAB, Uppsala
June 1991

TR 91-30
A resistance network model for radionuclide transport into the near field surrounding a repository for nuclear waste (SKB, Near Field Model 91)
Lennart Nilsson, Luis Moreno, Ivars Neretnieks, Leonardo Romero
Department of Chemical Engineering,
Royal Institute of Technology, Stockholm
June 1991

TR 91-31
Near field studies within the SKB 91 project
Hans Widén, Akke Bengtsson, Bertil Grundfelt
Kemakta Consultants AB, Stockholm
June 1991

TR 91-32
SKB/TVO Ice age scenario
Kaj Ahlbom[1], Timo Äikäs[2], Lars O. Ericsson[3]
[1]Conterra AB
[2]Teollisuuden Voima Oy (TVO)
[3]Svensk Kärnbränslehantering AB (SKB)
June 1991

TR 91-33
Transient nuclide release through the bentonite barrier - SKB 91
Akke Bengtsson, Hans Widén
Kemakta Konsult AB
May 1991

TR 91-34
SIMFUEL dissolution studies in granitic groundwater
I Casas[1], A Sandino[2], M S Caceci[1], J Bruno[1], K Ollila[3]
[1]MBT Tecnologia Ambiental, CENT, Cerdanyola, Spain
[2]KTH, Dpt. of Inorganic Chemistry, Stockholm, Sweden
[3]VTT, Tech. Res. Center of Finland, Espoo, Finland
September 1991

TR 91-35
Storage of nuclear waste in long boreholes
Håkan Sandstedt[1], Curt Wichmann[1], Roland Pusch[2], Lennart Börgesson[2], Bengt Lönnerberg[3]
[1]Tyréns
[2]Clay Technology AB
[3]ABB Atom
August 1991

TR 91-36
Tentative outline and siting of a repository for spent nuclear fuel at the Finnsjön site. SKB 91 reference concept
Lars Ageskog, Kjell Sjödin
VBB VIAK
September 1991

TR 91-37
Creep of OFHC and silver copper at simulated final repository canister-service conditions
Pertti Auerkari, Heikki Leinonen, Stefan Sandlin
VTT, Metals Laboratory, Finland
September 1991

TR 91-38
Production methods and costs of oxygen free copper canisters for nuclear waste disposal
Hannu Rajainmäki, Mikko Nieminen, Lenni Laakso
Outokumpu Poricopper Oy, Finland
June 1991

TR 91-39
The reducibility of sulphuric acid and sulphate in aqueous solution (translated from German)
Rolf Grauer
Paul Scherrer Institute, Switzerland
July 1990

TR 91-40
Interaction between geosphere and biosphere in lake sediments
Björn Sundblad, Ignasi Puigdomenech, Lena Mathiasson
December 1990

TR 91-41
Individual doses from radionuclides released to the Baltic coast
Ulla Bergström, Sture Nordlinder
Studsvik AB
May 1991

TR 91-42
Sensitivity analysis of the groundwater flow at the Finnsjön study site
Yung-Bing Bao, Roger Thunvik
Dept. Land and Water Resources,
Royal Institute of Technology, Stockholm, Sweden
September 1991

TR 91-43
SKB - PNC
Development of tunnel radar antennas
Lars Falk
ABEM, Uppsala, Sweden
July 1991

TR 91-44
Fluid and solute transport in a network of channels
Luis Moreno, Ivars Neretnieks
Department of Chemical Engineering,
Royal Institute of Technology, Stockholm, Sweden
September 1991

TR 91-45
The implications of soil acidification on a future HLNW repository.
Part I: The effects of increased weathering, erosion and deforestation
Josefa Nebot, Jordi Bruno
MBT Tecnologìa Ambiental, Cerdanyola, Spain
July 1991

TR 91-46
Some mechanisms which may reduce radiolysis
Ivars Neretnieks, Mostapha Faghihi
Department of Chemical Engineering, Royal Institute of Technology, Stockholm, Sweden
August 1991

TR 91-47
On the interaction of granite with Tc(IV) and Tc(VII) in aqueous solution
Trygve E Eriksen, Daquing Cui
Royal Institute of Technology, Department of Nuclear Chemistry, Stockholm, Sweden
October 1991

TR 91-48
A compartment model for solute transport in the near field of a respository for radioactive waste (Calculations for Pu-239)
Leonardo Romero, Luis Moreno , Ivars Neretnieks
Department of Chemical Engineering, Royal Institute of Technology, Stockholm, Sweden
October 1991

TR 91-49
Description of transport pathways in a KBS-3 type repository
Roland Pusch[1], Ivars Neretnieks[2], Patrik Sellin[3]
[1] Clay Technology AB. Lund
[2] The Royal institue of Techonology Department of Chemical Engineering, Stockholm
[3] Swedisch Nueclear Fuel and Waste Management Co (SKB), Stockholm
December 1991

TR 91-50
Concentrations of particulate matter and humic substances in deep groundwaters and estimated effects on the adsorption and transport of radionuclides
Bert Allard[1], Fred Karlsson[2], Ivars Neretnieks[3]
[1]Department of Water and Environmental Studies, University of Linköping, Sweden
[2]Swedish Nuclear Fuel and Waste Management Company, SKB, Stockholm, Sweden
[3]Department of Chemical Engineering, Royal Institute of Technology, Stockholm, Sweden
November 1991

TR 91-51
Gideå study site. Scope of activities and main results
Kaj Ahlbom[1], Jan-Erik Andersson[2],
Rune Nordqvist[2], Christer Ljunggren[2], Sven Tirén[2],
Clifford Voss[3]
[1]Conterra AB
[2]Geosigma AB
[3]U.S. Geological Survey
October 1991

TR 91-52
Fjällveden study site. Scope of activities and main results
Kaj Ahlbom[1], Jan-Erik Andersson[2],
Rune Nordqvist[2], Christer Ljunggren[2], Sven Tirén[2],
Clifford Voss[3]
[1]Conterra AB
[2]Geosigma AB
[3]U.S. Geological Survey
October 1991

TR 91-53
Impact of a repository on permafrost development during glaciation advance
Per Vallander, Jan Eurenius
VBB VIAK
December 1991

TR 91-54

Hydraulic evaluation of the groundwater conditions at Finnsjön. The effects on dilution in a domestic well

C-L Axelsson[1], J Byström[1], Å Eriksson[1],
J Holmén[1], H M Haitjema[2]
[1]Golder Geosystem AB, Uppsala, Sweden
[2]School of Public and Environmental Affairs,
Indiana University, Bloomington, Indiana, USA
September 1991